論文 / 著書情報
Article / Book Information

題目(和文)	二次元ナノ材料上における自己組織化ペプチドによるバイ オエレクトリック界面の動的形成の理解
Title(English)	Dynamic formation of bioelectronic interfaces by self-organized peptides on 2D materials
著者(和文)	関貴一
Author(English)	Seki Takakazu
出典(和文)	学位:博士(工学), 学位授与機関:東京工業大学, 報告番号:甲第11087号, 授与年月日:2019年3月26日, 学位の種別:課程博士, 審査員:早水 裕平,森 健彦,大内 幸雄,石川 謙,松本 英俊
Citation(English)	Degree:Doctor (Engineering), Conferring organization: Tokyo Institute of Technology, Report number:甲第11087号, Conferred date:2019/3/26, Degree Type:Course doctor, Examiner:,,,,
学位種別(和文)	博士論文
Category(English)	Doctoral Thesis
種別(和文)	要約
Type(English)	Outline

DYNAMIC FORMATION OF BIOELECTRONIC INTERFACES BY SELF-ORGANIZED PEPTIDES AND 2D MATERIALS

A dissertation submitted to the Tokyo Institute of Technology

For the degree of Doctor of Engineering

Takakazu Seki

TABLE OF CONTENTS

– Abstract –

This doctoral thesis entitled “Dynamic formation of bioelectronic interfaces by self-organized peptides and 2D materials” describes the effect of electrochemically biased environment on the behavior of self-organized peptides on two-dimensional (2D) nano-materials and development of a new bio-sensing platform to investigate the local molecular events at the interface between pseudo-biological environment and electronic semiconductor.

Boundaries between living systems and artificial systems, especially electronic devices are regarded as bioelectronic interfaces. One of long-standing scientists’ dreams in this research field is realization of bidirectional flow of biological signals by bridging the interface between electronic device and bio-modules such as functional proteins and living cells, where not only small molecules but also ions play significant roles. To date, primitive but successful demonstrations have been reported as exemplified by neuronal field-effect transistor devices and a variety of bio-sensing devices which have functional biomolecules responding to bio-related substances. In reality, surfaces of living cells are decorated with various type of functional molecules such as membrane proteins, and the functionalities and surrounding ionic environments do not have uniform geometry, which may be attributed to efficient cell-cell communications. Besides, such ionically uniform space may offer undulated two-dimensional ionic distribution which is difficult to be understood from the viewpoint of the traditional electrochemical double layer. However, despite the growing significances, there is still lack of the methodology to investigate the biological surface phenomena from the electronic point of view. To shed light on this topic, a bioelectronic model for pseudo-biological environment has developed, and using optical poperies of the 2D nano-material, ionic behavior and interactions between ions and the self-organized peptides at the interface have been investigated.

Firstly, the surface charge effect on surface behaviors of the self-organized peptide is discussed in chapter 2. The self-organized peptides have ability to form coherently ordered structure on various electronic materials surface and the coherent characteristics have been expected to act as molecular scaffolds for functional molecules on the device surface and also to offer a platform to study the effect of surface charges (potential) to the surface biomolecules. The first question toward understanding the bioelectronic interface is how the surface biomolecules behaves under the electrochemical bias and how much their organized structure is perturbed. To answer these questions here, an electrochemical cell composed of highly-oriented pyrolytic graphite (HOPG) and graphite-binding peptides (GrBPs) was made. Using this electrochemical cell, the self-organized structure under various electrochemical bias in water were investigated by atomic force microscope (AFM). The correlation between the amino-acids sequence of peptides and structural stability of organized mono-layer against applied electrochemical bias and also the effect of local pH on the peptide-organized structure are described.

Secondly, photoluminescence behavior of molybdenum disulfide (MoS_2) under pH-biased aqueous solution is described in chapter 3. MoS_2 is one of attractive layered materials, which belongs to a class of transition metal chalcogenide (TMD). Single layer MoS_2 has prominent

properties arising from the semi-conductive nature, e.g., strong photoluminescence (PL) and tunable electronic conductivity with a field effect transistor (FET) configuration. Large area crystal of MoS_2 and the PL behavior can be used for the spatial visualization of the complex behavior of the bioelectronic interfaces. However, compared to the FET-type MoS_2 application, optical sensing under aqueous condition application has not been demonstrated although MoS_2 has several advantages such as high sensitivity of optical behavior of MoS_2 to surrounding solvent and molecular adsorptions. The second questions here are how PL of MoS_2 is modulated and how MoS_2 PL response can be affected by surrounding ions. To address these questions, MoS_2 PL behavior was investigated by *in situ* PL measurement. The results revealed a large PL modulation by surrounding pH condition. The origin of this pH response was systematically studied with various types of MoS_2 using X-ray photoelectron spectroscopy and electron density analysis by PL measurements and a FET device.

Finally, using an electrochemical cell consisting of MoS_2 optical sensor and a gate electrode, time-dependent PL behaviors under various electrolyte solutions are investigated. PL was modulated with electrochemical pulse wave modulation. The modulated PL showed anomalously long decay behaviors, which is two or three orders of magnitude larger than the typical duration of the formation of electrical double layer, and the decay time constants were evaluated under aqueous solutions. Functionalization of MoS_2 surface with self-organized peptides largely affected the decay response to ions. These PL responses and the effects of biomolecular functionalization are described in chapter 4.

– Acknowledgements –

First of all, I am very grateful to my supervisor, Prof. Yuhei Hayamizu, who guided me through the PhD study. His patience, motivation, and enthusiasm on the bio-nano research field often helped me in all these years of research.

I appreciated the support of all members of Hayamizu lab.; Ms. Tomoko Oonishi, Ms. Li Peiying, Mr. Chen Chen, Mr. Takuma Narimatsu, Mr. Kazuki Yatsu, Mr. Yasuaki Nakata, Mr. Hironaga Oguchi, Mr. Sayaka Tezuka, Ms. Noa Koishihara, Mr. Kazumori Motai, and Mr. Chisyu Homma.

I also thank the support from former members; Mr. Tamon Page, Mr. David Starkebaum, Dr. Sun Linhao, Mr. Masujima Hiroaki, Mr. Hiroto Fukata, Mr. Morio Isoda, Mr. Kaito Sunamura, Mr. Tomohiro Tanaka, Mr. Shohei Tsuchiya, Mr. Kohei Sakuma, Mr. Tehoon Kim, Mr. Hiroyuki Kusumoto, Mr. Hayato Nonaka, and Mr. Adi.

I would like to thank the Research and Education Consortium for Innovation of Advanced Integrated Science (CIAiS), who gave me financial support during the period of my doctoral course.

Last but not least, I cannot imagine there is the word to describe how thankful I am to my parents and grandparents; Mr. Koichi Seki, Mrs. Fumie Seki, Mr. Michio Seki, and Mrs. Hanako Seki, who gave me excellent educations and chance to pursue PhD study at Tokyo Institute of Technology. Also I would like to show my gratitude to my fiancé, Fumika, who always supports my life.

This thesis would not be possible without the all supports above.

– List of Publications and Conferences –

Publications related to this thesis:

1. Seki, T.; So, C. R.; Page, T. R.; Starkebaum, D.; Hayamizu, Y.; Sarikaya, M. "Electrochemical Control of Peptide Self-Organization on Atomically Flat Solid Surfaces: A Case Study with Graphite", *Langmuir* **2018**, *34*, 1819–1826.

Conferences:

1. Takakazu Seki, Kazuki Yatsu, Yuhei Hayamizu, and Mehmet Sarikaya. Electrochemical modulation of MoS_2 photoluminescence behavior in various electrolyte aqueous solutions for potential biological sensing, 4th Edition of the European Graphene Forum - EGF 2018, Venice, Italy, Oct.2018 (Oral)

2. Takakazu Seki, Christopher R. So, Tamon R. Page, David Starkebaum, Kazuki Yatsu, Kaito Sunamura, Yuhei Hayamizu, and Mehmet Sarikaya. Electrochemical modulation of peptides organization on two-dimensional materials, The First International Workshop by the 174th Committee JSPS on Symbiosis of Biology and Nanodevices, Kyoto, Japan, Dec.2017 (Poster)

3. Takakazu Seki, Christopher So, Tamon Page, David Alan Starkebaum, Yuhei Hayamizu, Mehmet Sarikaya. Electrochemical control of peptide self-organization on graphite surfaces, 2017 MRS Fall Meeting & Exhibit, Boston, US, Nov.2017 (Poster)

4. Takakazu Seki, Christopher R. So, Tamon R. Page, David Starkebaum, Kazuki Yatsu, Kaito Sunamura, Yuhei Hayamizu, and Mehmet Sarikaya. Electrochemical modulation of peptides organization on two-dimensional materials, 5th Ito International Research Conference, RIKEN Centennial Anniversary & Surface and Interface Spectroscopy 2017, Tokyo, Japan, Nov.2017 (Poster)

5. Takakazu Seki; Christopher So; Tamon Page; David Starkebaum; Kazuki Yatsu; Kaito Sunamura; Yuhei Hayamizu; Mehmet Sarikaya. Electrochemical control of peptides self-assembling behavior on 2D nanomaterials, Graphene Week, Athens, Greece, Sep.2017 (Poster)

6. Takakazu Seki, Kazuki Yatsu, Yuhei Hayamizu. Electrical Modulation of Single-layer MoS_2 Photoluminescence under Aqueous Electrolyte Solution for Potential Biological Sensing, The 79th JSAP Autumn Meeting/JSAP-OSA Joint Symposia 2017, Fukuoka, Japan, Sep.2017 (Oral)

7. Takakazu Seki, Christopher R. So, Tamon R. Page, David Starkebaum, Kazuki Yatsu, Kaito Sunamura, Yuhei Hayamizu, and Mehmet Sarikaya. Response of peptide layer on electrochemical transistor of MoS_2 characterized by photoluminescence, The 79th JSAP Autumn Meeting, Fukuoka, Japan, Sep.2017 (Oral)

8. Takakazu Seki, Tomohiro Tanaka, Yuhei Hayamizu. Formation of planer lipid bilayers on 2D nano-materials assisted by self-assembled peptides, 9th International Conference on Molecular Electronics and Bioelectronics, Kanazawa, Japan, Jun.2017 (poster)

9. Takakazu Seki. Formation of Planer Lipid Bilayers on 2D Materials Assisted by Self-assembled Peptides, Donghua University – Tokyo Institute of Technology Joint Symposium on Materials Science and Engineering, Tokyo, Japan, Jun.2017 (oral)

10. 関 貴一, 田中 智大, 早水 裕平. 自己組織化ペプチドを用いた二次元ナノ材料上への脂質二重膜展開, 35th CHEMINAS/化学とマイクロ•ナノシステム学会３５回研究会, 東京, 2017 年 5 月 (poster)

11. Takakazu Seki, Yuhei Hayamizu, Photoluminescence of MoS_2 modified by pH and ions in aqueous solutions for potential biological sensing, The 64th JSAP spring meeting 2017/ Joint Symposium on Nanobiotechnology and Biosensing, Yokohama, Japan, Mar.2017 (Oral)

12. Takakazu Seki, Tomohiro Tanaka, Yuhei Hayamizu. Formation of planer lipid bilayers on 2D materials assisted by self-assembled peptides, 2017 TMS, San Diego, California, US, Feb-Mar.2017 (Oral)

13. Takakazu Seki, Christopher So, Tamon Page, Yuhei Hayamizu, Mehmet Sarikaya. An Electrochemical Approach to Control Surface Behavior of Peptides Self-assembling on Graphite, 2016 TMS, Nashville, Tennessee, US, Feb.2016 (Oral)

14. Takakazu Seki, Tamon Page, Yuhei Hayamizu. An electrochemical control of peptides self-assembling behavior on graphite, Joint Symposium of the Surface Sience Society of Japan and the Vacuum Society of Japan, Tsukuba, Japan, Dec.2015 (Oral)

15. Takakazu Seki, Yuhei Hayamizu. Morphological Control of peptide self-assembly on graphite by electrochemically applied surface potential, International Symposium on Organic and Polymeric Materials – On Occasion of the 60th Anniversary of Department of Textile Engineering, Tokyo, Japan, Oct.2015 (Poster)

16. Takakazu Seki, Tamon Page, Yuhei Hayamizu. Self-organized peptides on highly ordered pyrolytic graphite tuned by electrochemically applied surface potential, The 76th JSAP Autumn Meeting, Nagoya, Japan, Sep.2015 (Oral)

– Abbreviations –

Aβ	Amyloid beta protein
AFM	Atomic force microscopy (microscope)
aq	Aqueous solution
arb. unit	Arbitrary unit
BN	Boron nitride
CVD	Chemical vapor deposition
CV	Cyclic voltammetry
CV-PL	PL measurement under cyclic modulation of electrochemical potentials
CW	Continuous wave (laser)
°C	Degrees Celsius
DI water	Deionized water
DNA	Deoxyribonucleic acid
EMCCD	Electron-Multiplying Charge-Coupled Device
eV	Electron volt(s)
FET	Field effect transistor
FFT	Fast Fourier transform
GrBP	Graphite binding peptide
HOPG	Highly ordered pyrolytic graphite
h	Hour(s)
h	Planck's constant
$\hbar$	Dirac's constant
MoS_2	Molybdenum disulfide
OC	Open circuit
PDMS	Poly(dimethylpolysiloxane)
PI	Isoelectric point
PL	Photoluminescence
PMMA	Poly(methyl methacrylate)
PS	Polystyrene
PVD	Physical vapor deposition
ROI	Region of interest
rt.	Room temperature
sccm	Standard Cubic Centimeter per Minute
S/N	Signal to noise ratio
T	Temperature
TMD	Transition metal dichalcogenide
UV	Ultraviolet
Vg	Gate voltage
Vth	Threshold voltage
XPS	X-ray photoelectron spectroscopy

CHAPETR 1. General Introduction

1.1 Bioelectronic interfaces

Bridging the boundary between artificial materials (machinery) world and living organism world is one of the most fascinating topics for mankind, not only for scientists. The ideas such as communicating living organisms and developing artificial organisms have been recognized for a long time and widely prevailed. Interestingly, such ideas have been found even in fictional characters, including Golem and Frankenstein.[1] What is important for this is realization of bidirectional flow of information between living world and artificial materials world. The place where the two-way communications occur can be defined as a "bioelectronic interface". To date, utilizing inorganic electronic materials, scientists have been trying to realize such communications through electron current, electric fields, and so forth. In the early stage of the realization of the vision, relatively large silicon field-effect transistor (Si-FET) devices have been employed to monitor neuronal activity of cells (**Figure 1**).[2,3] They have successfully demonstrated mono-directional flow of a biological information, a signal-read out from a living cell using a man-made device. Such a man-made device reading a signal, flow of ions/molecules is usually called a bio-sensing device.

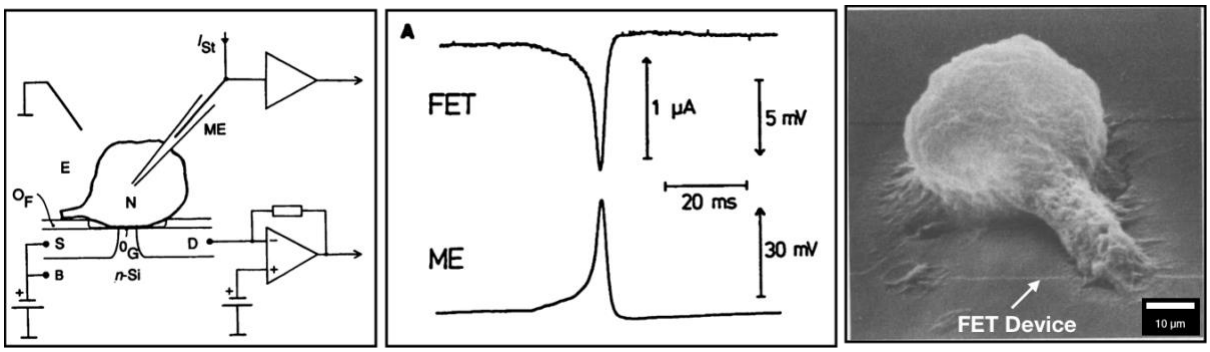

Figure 1. Schematics of neuron-Si FET junction, single action potential measured by a Si FET source-drain current, and electron microscope image a neural cell and a FET device. These figures are reprinted from ref. *2* with permission from AAAS.

After a while, the rise of nanotubes and nanowires structure such as carbon nanotube and Si nanowire and the establishment of the production methods have encouraged scientists to develop noble bioelectronic interfaces.[4,5,6] Such low dimensional materials have high surface-to-volume ratios, which enables high sensitivity compared to the traditional large planar devices, such as single molecular sensitivity. Recently, another type of electronic material with low dimensionality, i.e., graphene has appeared. Graphene consists of a single-atomic-layer of sp^2-bonded carbon atoms, and the physical properties of graphene electronic device have been intensively investigated.[78] Graphene devices, of course, have been subjected

to the bioelectronic fields. Scientists have demonstrated molecular/ion detection and also measured a signal produced by cells.[9,10,11,12] Reference 11 evaluated the utility of the graphene FET device and concluded that the graphene device has similar sensitivity to that of one-dimensional materials (**Figure 2**-(a)). Interestingly, in reference 11, they recorded cell signals using graphene FET array and found that the graphene FET array showed a variety of signal patterns (**Figure 2**-(b)). This can be attributed to the variation in the junctions formed between cells and graphene due to the existence of spatially dispersed membrane proteins and contact points onto the surface. This observation implicates that real bioelectronic interface offers undulated environments in terms of cell structure and molecular/ionic flow. In particular, the latter one such as the flow of chemical mediators/ions released from cells is considered to involve in the cell-cell communications. At such complex interfaces, the ionic distribution or kinetic behavior may be affected by not only charged device surfaces but also highly hydrated biomolecules/cells and may not follow the traditional electrochemical double layers such as Helmholtz model, Gouy-Chapman model, and Stern model, which have been believed by electrochemists and described typically as one-dimensional picture (**Figure 3**).[13,14] The local interfacial electrochemical behaviors are worth in-depth research from both fundamental and application points of view. To date, various method including optical approaches such as X-ray/non-linear optics sum-frequency generation and probe microscopic technique, have been employed to study water molecules and ions at liquid/solid interfaces.[15,16,17] However, despite the primitive successes, the surface-specific tools to investigate the molecular/ionic behaviors at the bioelectric interface are still limited such as Raman spectroscopy and plasmonic imaging due to the spatial confinement.[18,19]

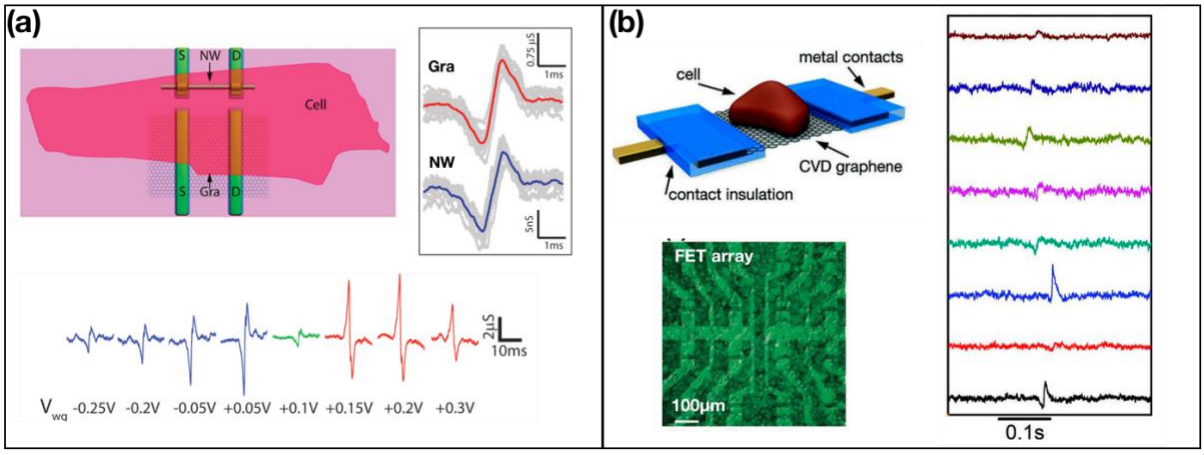

Figure 2. Graphene FET devices measuring cell signals. (a) compares the utility of nanowire-based FET and graphene FET and shows biphasic signal recordings by graphene FET. Reprinted with permission from ref. 11. Copyright 2011 American Chemical Society. (b) shows cell signals recorded by a graphene FET array. Reprinted with permission from ref. 12 Copyright 2012 Wiley.

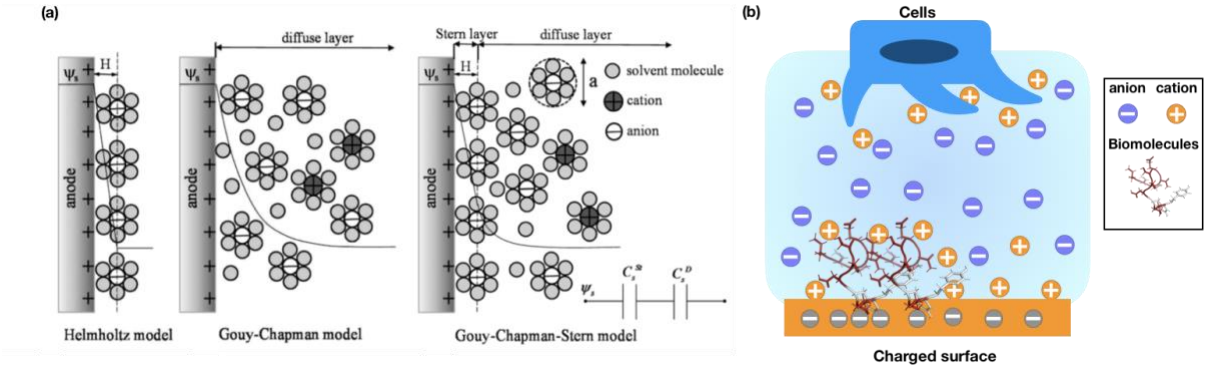

Figure 3. (a) Schematic illustration of electrochemical double layers according to Helmholtz model, Gouy-Chapman, and Stern models. Reproduced from Ref. 13 with permission from the Royal Society of Chemistry. (b) Schematics of the ionic distributions at the bioelectric interfaces formed with surface biomolecules and cells.

As for the opposite flow of biological information, one of promising approaches is utilizing intrinsic biological functionalities such as membrane proteins and enzymes.[20] The First step in this field is how to catch the functional bio-modules in action on the electronic device surface since sometimes hydrophobic nature of the nanomaterials induces protein denaturing. A practical way to construct the bio-modules on the surface of the electronic materials in a more natural manner is protein-conjugation via lipid membrane as proposed by Steinhoff and co-workers in early 2000s.[21] Recently, the several types of protein-conjugation on the nanomaterials such as Si nanowires and graphene have been demonstrated by many researchers successfully.[22,23,24,25] Despite these initial successes, there still seem to be tremendous steps toward efficient control of the bio-modules as living systems always do. To facilitate the bridging between the biological world and the artificial, the surface phenomena should be understood further from the fundamental aspects.

1.2 Focus of this thesis

In this thesis, to understand the complex behavior of the bioelectronic interface from the viewpoint of electronic coupling between the device and biomolecules, I have developed model bioelectronic interfaces consisting of self-organized peptides and recently emerging 2D nanomaterials (**Figure 4**).

Proteins/enzymes are often utilized to functionalize the electronic device surfaces to establish directed-flow of information from biological world. Although such functional macro-biomolecules have very fascinating properties, there are still several difficulties in controlling surface orientation and functions, which may make the situation more difficult to be understood. In stark contrast, the recently developed self-organized peptides are considered to have coherently organized surface structure ideally, which enables efficient exploration of the electronic (surface) effect from the device to the bio-modules. In chapter 2, by employing an

electrochemical cell consisting of the self-organized peptides and a graphite electrode, surface structures formed by the self-organized peptides are investigated under electrochemical biases.

To study the reversely-directed effect from the bio-modules and surroundings to the device, optical properties of the 2D material has been employed. In chapter 3, optical responses of molybdenum disulfide under electrolyte solutions are explored. Chapter 4 also describes optical responses to aqueous ionic environments. In this chapter, an electrochemical cell with molybdenum disulfide is developed and optical responses to ions/water are discussed from a kinetic aspect under electrochemical biases. Besides, effects of self-organized peptide layer on the optical responses are debated. The details about the self-organized peptides and the emerging 2D nanomaterials are described below.

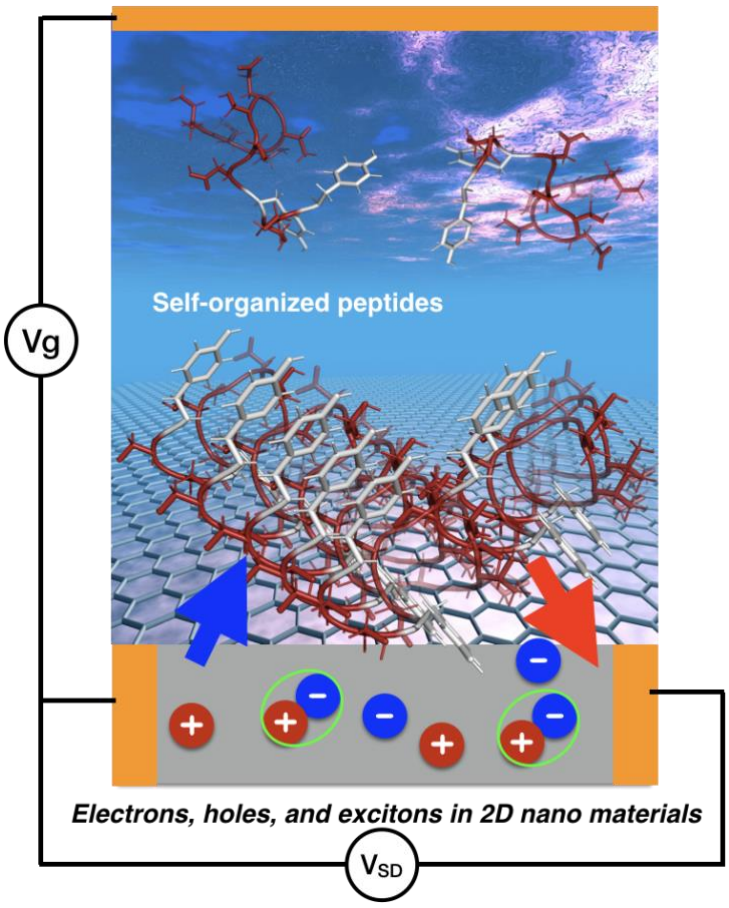

Figure 4. Schematic illustration of the bioelectronic interface consisting of the self-organized peptides and the 2D nanomaterial with a device configuration. The blue and red arrows indicate the bidirectional communications between the bio-modules and electronic/excitonic quasiparticles.

1.3 Self-organized peptides on a solid surface

There is a long and rich research history of the bio-molecular self-assembly, which mainly describes "soft" supramolecular structures in a solution phase, including vesicles and micelles formed by lipid molecular layer, DNA complexation, and also macroscopic structure formation by anisotropic interaction between proteins toward understanding how living organisms appear and perform complex functions.[26] At the same time, people have been gaining inspiration for the design and the functions of biomolecules from nature, which has been creating a variety of hybrid smart structure of the living organisms (**Figure 5**).[27,28,29] In these examples, the nature takes advantages of not only the anisotropic feature of the biomolecular assembly but also hard characteristics of inorganic materials to create mesoscopic to macroscopic objects. These "hard" assemblies (organizations) have been intensively studied in the field of biomimetics.

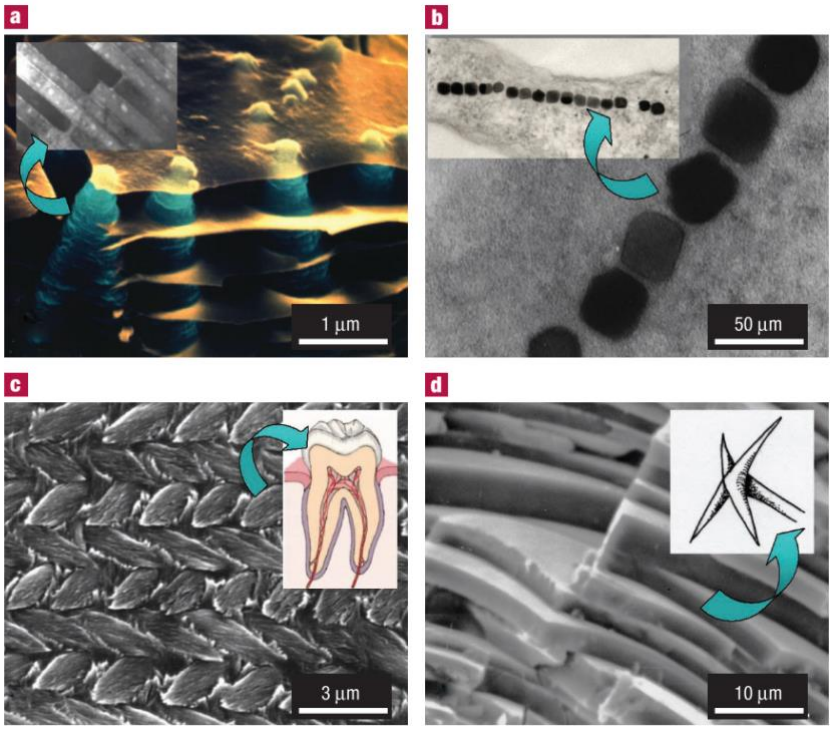

Figure 5. Electron microscopic images showing the examples of biologically created complex structure consisting of soft biomolecules and hard inorganic materials. Reprinted by permission from ref. 29.

Among the "hard" self-assembly (organization), self-organization behaviors of proteins on a solid have been attracting much attention since the discovery of the formation of self-organized structure with amyloid beta proteins (Aβ) by Kowalewski and Holtzman in 1999 (**Figure 6**).[30] They expected that some proteins undergo structural conversion from water-soluble α (alpha)-helix species to insoluble β (beta)-sheet species in a biological condition at some point and that the conversion induce the undesired protein aggregation, which may be attributed to the cause of diseases such as Alzheimer's disease and Huntington's disease.[31,32,33] On this hypothesis, using in-situ atomic force microscope (AFM) measurement, they investigated structural conversion of Aβ induced by a solid surface and found the Aβ formed highly ordered surface structure reflecting a six-fold symmetric feature of the surfaces, mica and highly ordered pyrolytic graphite (HOPG).

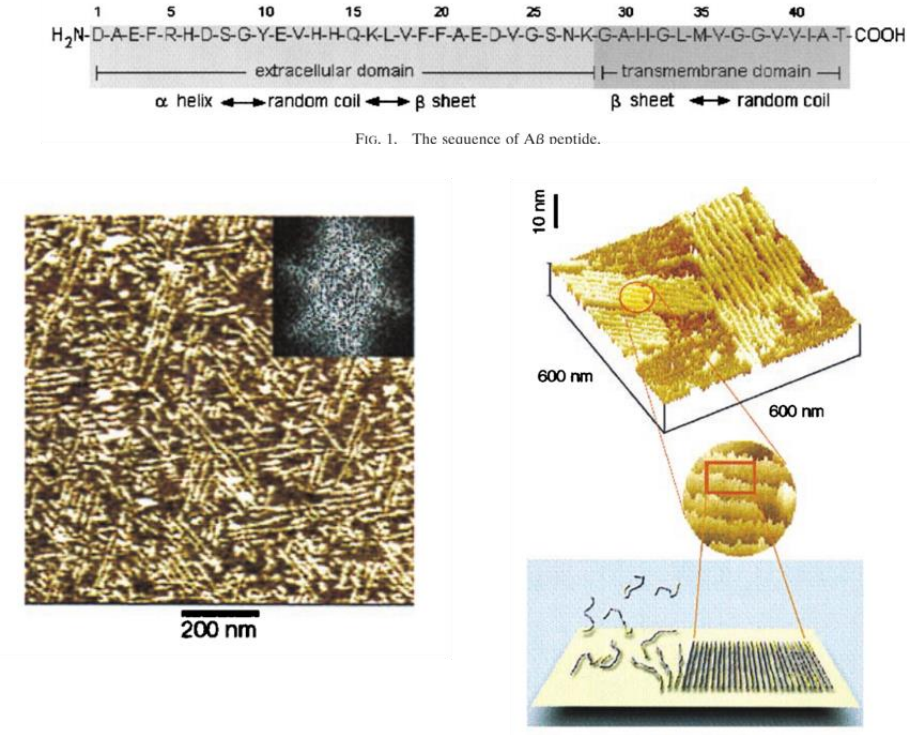

Figure 6. The amino acid sequence of Aβ protein and AFM images of the self-organized structure on graphite surface.[30] Copyright 1999 National Academy of Sciences.

After the demonstration of the self-organization behavior of the Aβ protein, to further understand correlations between amino acid sequence and the organization behavior, various peptides and proteins have been subjected.[34,35,36] In particular, GAV-9 peptide having a hydrophobic amino-acid sequence of VGGAVVAGV with an amidated C-terminus is one of the most studied self-organized peptides.[36,37] This amyloid-like hydrophobic peptide showed highly-ordered nano-wires in three preferential orientation at 120° to each other. The feature

of the organization structure was affected by the hydrophilicity of the substrates. While the hydrophilic surface (mica) offered "up-right" orientation of the peptides, the peptides formed "edge-on" orientation on the hydrophobic substrate (HOPG) as shown in **Figure 7**. This orientation behavior can be understood in terms of the hydrophobic interactions between the peptide and the substrates.

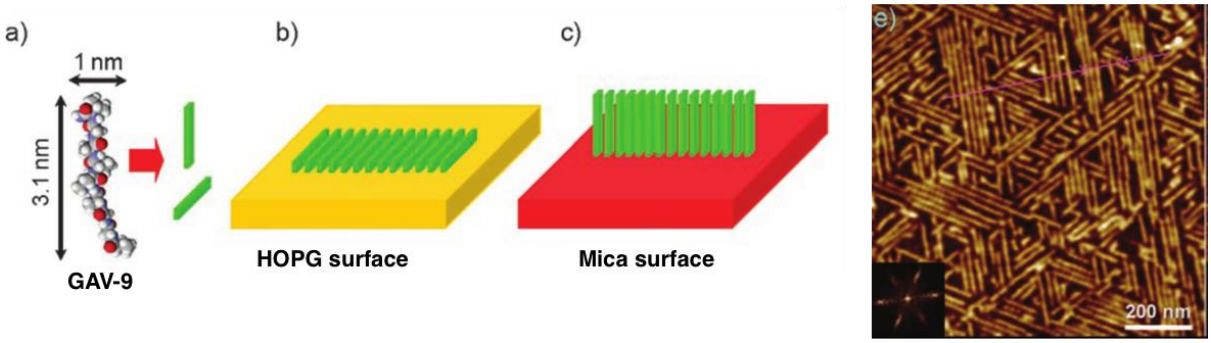

Figure 7. Schematic representation of GAV-9 peptide and its self-organization on HOPG and Mica substrates, and AFM image of the organization behavior on HOPG. Reprinted from ref. 36. Copyright 2006 WILEY-VCH Verlag GmbH & Co. KGaA, Weinheim.

In the last decade, aiming to develop nano-bioelectronic devices based on the self-organized peptides, people made considerable strides on the peptides' organization on graphite/graphene, which can be a promising base material for the electronic/electrochemical applications.[38,39,40,41,42] The behavior of these peptides on solid surfaces has also been investigated theoretically using computational modeling.[43,44,45] While many peptides have been developed the self-organized peptides *de novo* (from scratch) or inspired by naturally occurring proteins, graphite binding peptides (GrBPs) have been selected by a phage-display method. The amino-acid sequence and the self-organization behaviors of the original GrBP (GrBP-WT) are shown in ***Figure 8***. The GrBP-WT is also able to self-organize into the highly-ordered surface structure as other peptides can. The self-organized layer usually shows around 1nm-thickness, indicating the mono-molecular layer. This peptide has 12 amino acids in their sequence, which can be categorized into three parts: (i) hydrophobic part (IMV), (ii) hydrophilic part (TESSD), and (iii) aromatic-rich part (YSSY). It was found that these domains play important roles in the organization behavior. A modification of the amino acid sequence in the aromatic-rich part, e.g., from tyrosine to alanine, weakened the binding affinity to the surface, which can be explained by lack of major binding interaction, π-π interaction. Interestingly, a substitution of the hydrophobic amino acids with hydrophilic amino acids cause disorganization of the surface structure. From this observation, it can be concluded that the amphiphilic module consisting of domain (i) and (ii) is indispensable for the formation of the well-organized structure.

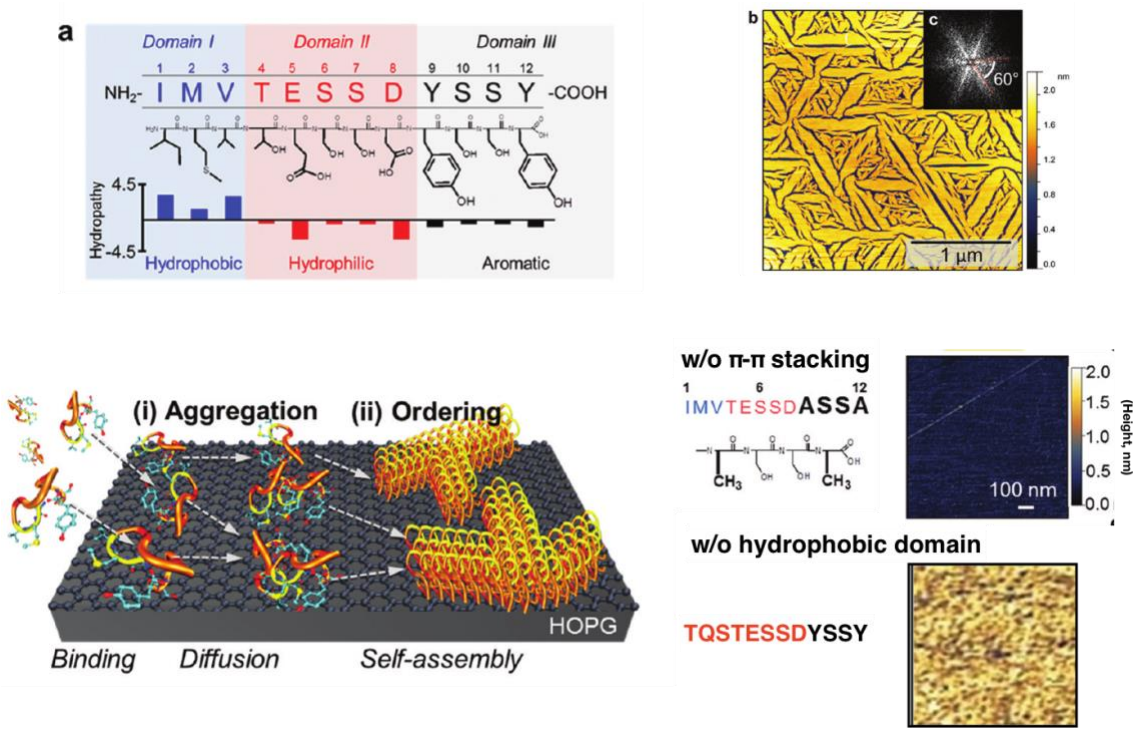

Figure 8. Amino acid sequence of the GrBP wild type and its self-organization behavior on graphite surface. Reprinted with permission from ref. 38. Copyright 2013 American Chemical Society.

Recently, modulation of electrical properties of graphene by the self-organized peptides has been demonstrated with a field effect transistor (FET) device configuration.[46,47] They decorated the surface of a graphene FET with biotinylated GrBP and demonstrated detection of a target protein via a specific interaction between biotin and streptavidin as a resistance decrease in between two electrodes (**Figure 9**). Although many demonstrations on FET type sensing of biomolecular binding have been performed, the mechanism of the detection is still under debate.[48] Among several suggested mechanisms, two effects such as electrostatic gating and Schottky barrier effects are considered to be dominant.[49] In a similar way, it was found that the self-organized layer of GrBP itself affected the electrical conductivity of a graphene FET (**Figure 10**). The electrical conductivity can be modulated by a gate applied voltage. After the formation of the peptide-organized layer on it, the conductivity modulation showed two distinct peaks, namely W-shape response, different from the original V-shape response to the gate voltage. The gate response was largely affected by a surface coverage of the peptide layer. As the coverage increased, As the coverage increased, the ordered domain became larger. Along with an increase in the ordered domain, the W-shape response gradually diminished, and the gate response showed the V-shape response finally with a large peak shift, which indicates negatively-charged peptide caused hole-doing into the graphene. This observation has important implication that the organized structure by GrBP on the device does not impair the intrinsic electronic properties.

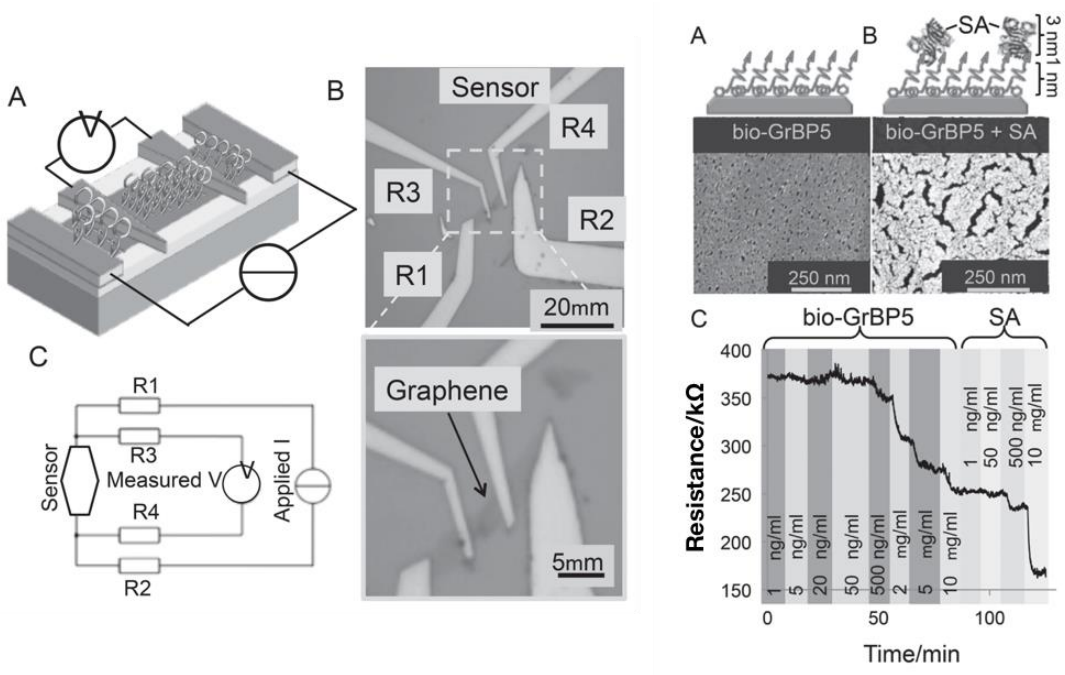

Figure 9. Schematic illustration of GrBP-coated FET device and demonstration of protein-detection via specific binding with ligand-modified GrBP. Reprinted from ref. 46. Copyright 2014 WILEY-VCH Verlag GmbH & Co. KGaA, Weinheim.

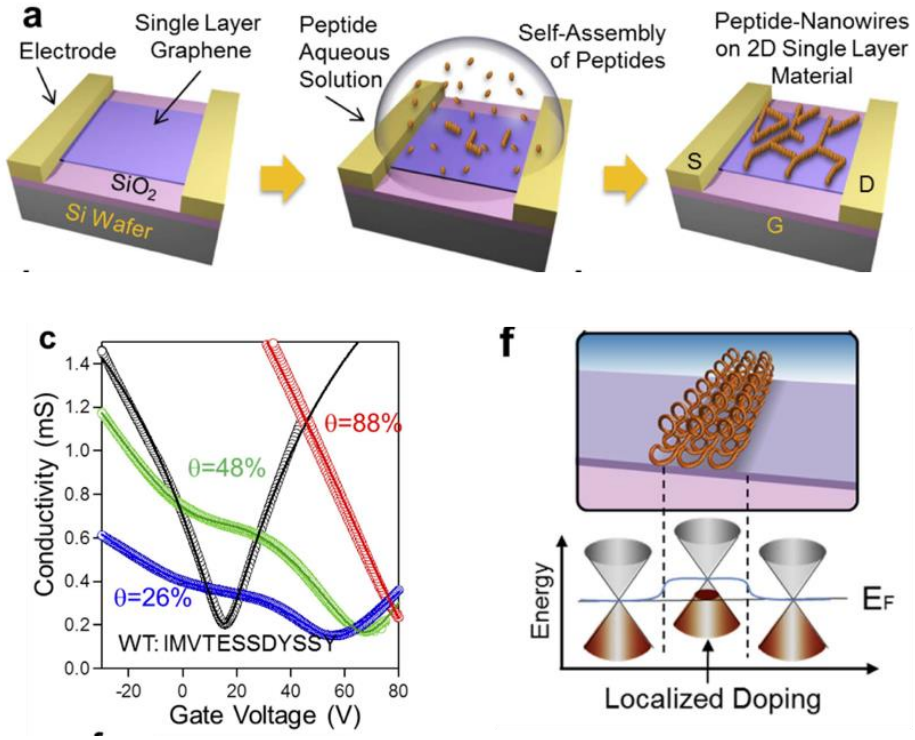

Figure 10. illustration of the formation of the self-organized layer of GrBP on a surface of a graphene FET device and modulation of electrical conductivity of the graphene device. [47]

Interestingly, by applying amino acid variation in the sequence, GrBP variants can form the organized structure even on other two-dimensional (2D) layer materials such as molybdenum disulfide (MoS_2), tungsten diselenide (WSe_2), boron nitride (BN), and so forth (**Figure 11**-(a)).[47] More recently, it has been reported that other type of peptides also forms the organized structure on the MoS_2 surface.[50,51] One of the MoS_2 binding peptides, MoSBP1 formed highly organized surface structure, which is confirmed by *in situ* AFM (**Figure 11**-(b)). To date, the spectrum of the self-organized peptide layer has been extending in wide range of two-dimensional materials including, metal, semi-metal, semiconductor, and insulator, which offer great opportunities for the formation of versatile platform toward the future bio-electronics.

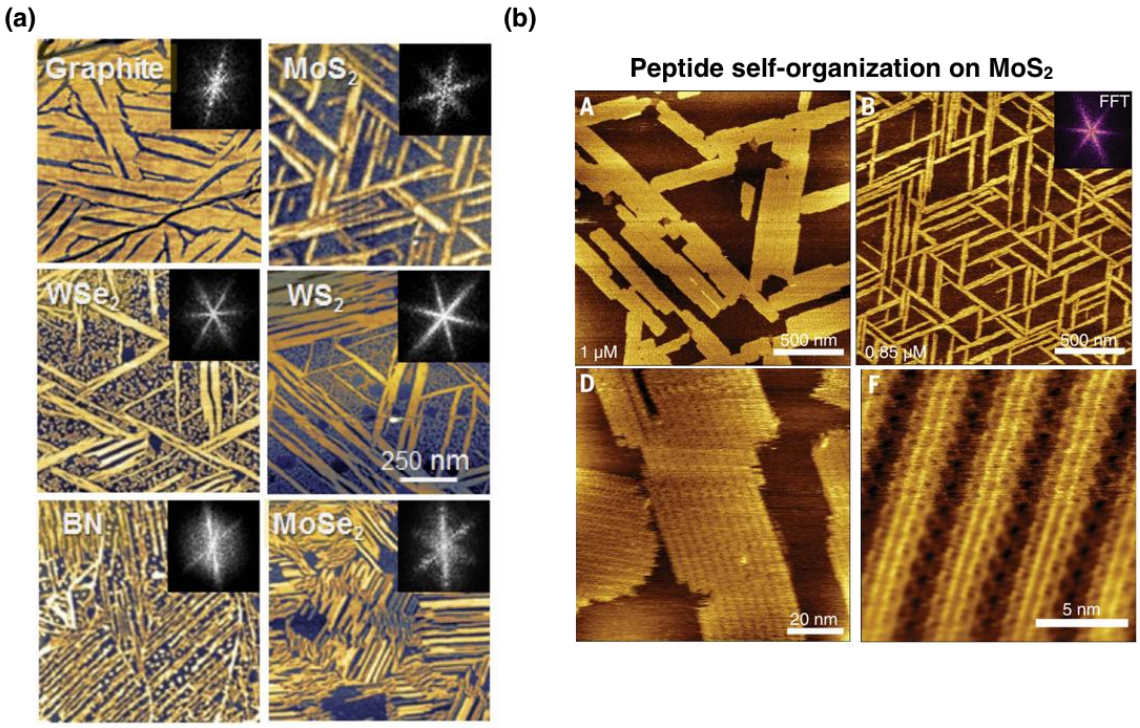

Figure 11. (a, b) AFM images of a variety of solid binding peptides having the self-organization capability, GrBP series (a)[47] and MoSBP1 (b). These figures are reprinted from ref. 51 with permission from AAAS.

1.4 Two dimensional layered materials

Ultra-thin 2D materials have been gaining much attention as post-Si devices due to their unique-optoelectronic properties and also feasibility in fabricating complex structure with a large area compared to 1D nano-materials.[52,53,54] A boom in the field of 2D layered materials have started from the first isolation of graphene, monolayer counterpart of graphite, and following findings of a family of 2D materials, which can also be isolated by the tape-exfoliation method.[55,56] The isolated these monolayer materials exhibit extraordinarily different properties from those of the bulk counterparts. Among them, MoS_2, one of the transition metal dichalcogenides (TMDs), has been regarded as the flagship material beyond graphene. The bulk MoS_2 is an indirect bandgap material with a band gap of 1.29 eV, and having a build-up structure comprising of three atom layers of S-Mo-S via weak van der Waals interaction.[57,58,59] (**Figure 12**-(a,b)). Very interestingly, when reducing the number of layers, MoS_2 underwent indirect-to-direct-bandgap crossover gradually due to perpendicular quantum confinement, and single-layer (SL)- MoS_2 exhibited pronounced photoluminescence (PL) upon light excitation (**Figure 12**-(c,d)).[60,61,62,63] In the case of few-layer, MoS_2 showed weak PL attributed to indirect bandgap transition in the range of 1.4-1.6 eV.

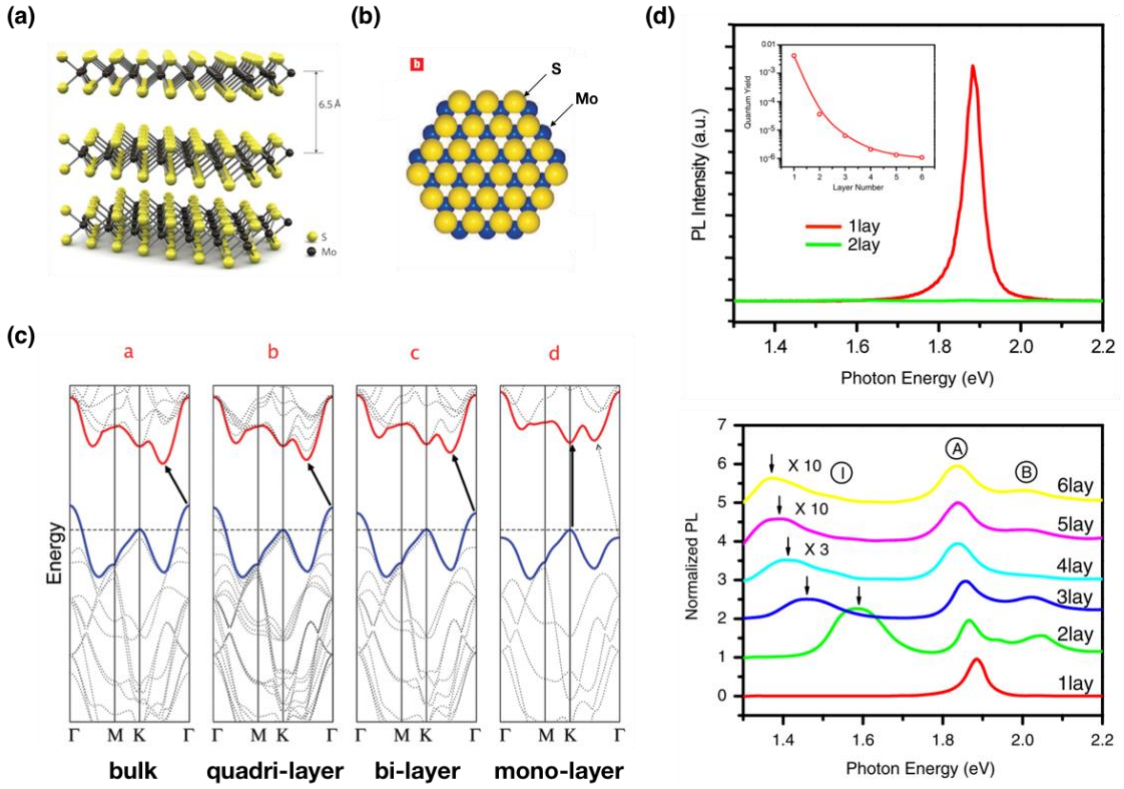

Figure 12. (a, b) Schematic illustration of typical MoS_2 layer structure form side (a) and from top (b). Reprinted with permission from ref. 58 and 59, respectively. (c) Calculated layer-dependent band structures of MoS_2. Reprinted with permission from ref. 60. Copyright 2010 American Chemical Society. (d) PL spectra of MoS_2 with different layer thickness. Reprinted with permission from ref. 61. Copyright 2010 by the American Physical Society.

Due to the bandgap and relatively high carrier mobility, semiconducting 2D materials have gained increasing attention as promising channel part for FET device, phototransistor, and photodetector since successful demonstrations with SL-MoS_2.[58, 64 , 65 , 66 , 67] Since the emergence of such sensitive FET device with new generation 2D materials beyond graphene, MoS_2 FET device have been intensively employed for biomolecular detection toward bioelectronic applications due to the sensitive electronic nature as well as biocompatibility (**Figure 13**).[68,69,70] In reference 68, they fabricated a MoS_2 FET and modified the surface with dielectric oxide layer. Firstly, they demonstrated pH-sensing based on the protonation/deprotonation mechanism of hydroxy groups on the gate dielectric layer, modulation of the surface charge depending on the pH in electrolyte solutions. Further surface modification with biotin probe via silane coupling and well-known biotin-avidin interaction enabled the detection of the target protein in an efficient manner. At the solution pH below the isoelectric point (PI) where molecule has net neutral charges, avidin was negatively-charged, and the current between the source/drain electrodes decreased. On the other hand, the binding of avidin at the solution pH above the PI value increased the current. These changes were attributed to shifts of threshold voltage of the transistor, which is consistent with the charge-nature of the protein. In the case of reference 69, they immobilized probe molecules directly on the MoS_2 surface to reduce a special distance between MoS_2 and charged biomolecules since screening of the biomolecules by the ionic environment can deteriorate the device sensitivity.[71] They also demonstrated biomolecular detections via antigen/antibody interaction. These works are successful examples of the detection of the interaction between biomolecules and the electronic materials although still the mechanism is under discussion.[72]

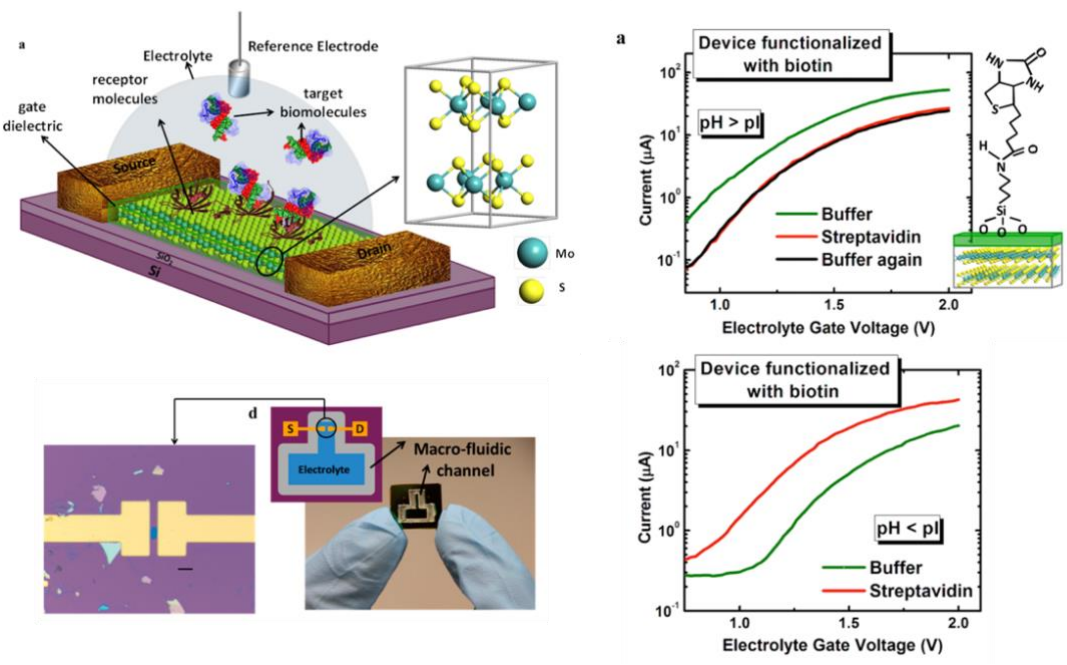

Figure 13. Biosensing MoS_2 FET device and current modulation by protein adsorption. Reprinted with permission from ref. 68. Copyright 2014 American Chemical Society.

Aside from the sensitive electronic applications of TMDs, unique luminescence properties are also worth in-depth investigation. As mentioned above, SL-TMDs showed pronounced PL due to quantum mechanical confinement. The quantum confinement gives rise to tightly-bound excitons (a bound state of one electron and one hole, in other words, an electron-hole-pair) with extremely large binding energy, ranging from 200meV to 900meV, especially for SL-MoS_2.[73,74,75,76] This tight-binding phenomenon on the formation of excitons causes mismatching between the electronic bandgap and the optical bandgap which is usually consistent with the electronic bandgap. The evidence of the excitonic effects in these ultrathin 2D materials was provided by the experimental absorption spectrum with sharp resonance features as shown in (**Figure 14**-(a)).[60,61] In the absence of the excitonic features, the absorption spectrum of 2D materials is generally characterized with a step-like function from the joint-density-of-state function.[77] Besides, the confined effect further induces higher order of excitonic states such as trion (a bound state of two electrons and one hole, or one electron and two holes) (**Figure 14**-(b)).[78,79] What is truly intriguing is that observation of the excitonic quasi-particles even at room temperature due to that much large binding energy compared to the thermal energy (k_BT at room temperature) of 25.9 meV. This has been providing many possibilities of room-temperature excitonic applications and exploration of 2D physics in various fields.

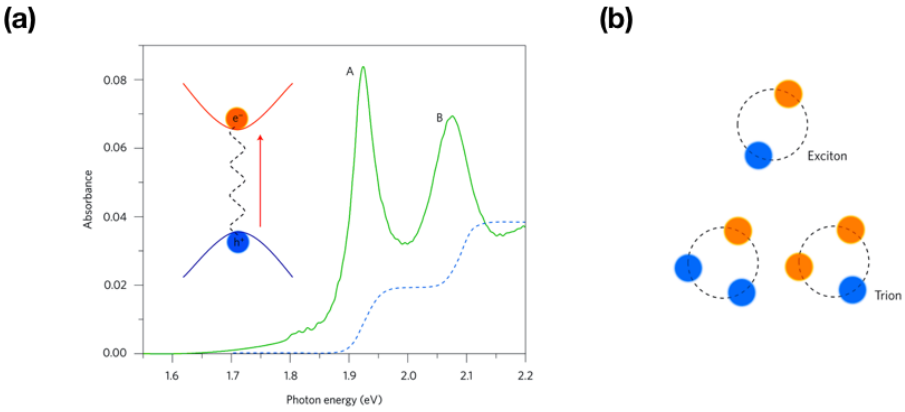

Figure 14. (a) Absorption spectrum of SL-MoS_2 at 10 K. The blue line indicates the absorption spectrum in the absence of the excitonic feature. (b) Schematic illustration of the excitonic states of exciton and trion. Reprinted with permission from ref. 53.

The stable excitonic quasiparticles at room temperature have driven many researchers to investigate interplays between exciton/trion and charge carriers to pave the way for controlling optical properties of TMDs, in particular, MoS_2. These investigations revealed that the excitonic quasiparticles are highly sensitive to external environmental factors such as electric field, molecular adsorption, and surrounding dielectric materials due to the high surface-to-volume ratio.[78,80,81,82] In reference 78, by inducing charged carrier into SL-MoS_2 with the application of the gate voltage, they found that another excitonic resonance appeared

having lower energy in the absorption spectrum under positive gate voltage (electron rich condition), and assigned the newly appeared resonance as the higher-order excitonic state, trion possessing a large binding energy (~20 meV). The experimentally obtained trion binding energy was compatible with estimated trion energy (~1/10 of exciton binding energy).[83] The PL attributed to these excitonic states were affected by the carrier density (**Figure 15**-(a)). As increasing the carrier density in MoS_2, the PL attributed to exciton was suppressed while the PL attributed to trion showed constant contribution over the range of the gate voltages, leading to the trion-dominant situation in the PL. Importantly, they also reported that the PL modulation was not observed at 10K where the dominant PL came from the pre-equilibrium state of exciton and trion and claimed that exciton PL originally excited from the trion state at the primary stage. In reference 80, they also achieved the PL modulation by chemical doping method as a substitute for using complex device structure such as FET configuration. The chemical doping is well known to modulate carrier density in the field of graphene.[84,85] The idea is based on the charge-transfer between dopant molecules and the electronic materials to induce a shift in the Fermi level. In this paper, they demonstrated p-type doping with 2,3,5,6-tetrafluoro-7,7,8,8-tetracyanoquinodimethane (F4TCNQ) and 7,7,8,8-tetracyanoquinodimethane (TCNQ) and also n-type doping with nicotinamide adenine dinucleotide (NADH) on SL-MoS_2 (**Figure 15**-(b)). Upon adsorption of p-type chemical dopants, the PL attributed to exciton was largely enhanced whereas adsorption of n-type chemical dopant suppressed the PL contribution. Similarly to reference 78, the trionic PL intensity was unaltered regardless of increasing the number of chemical doping. Both two investigations successfully proved tunability of the excitonic and trionic PL in SL-MoS_2.

It is also reported that the PL of SL-MoS_2 has substantial correlations with the surrounding solvents and dielectric environments. In reference 81, they investigated shifts in the PL energy under various solvents. The energy shift in the emission or the absorption by surrounding solvents is traditionally called "solvatochromism", which have been widely studied for fluorophores, quantum-dot, and carbon-nanotube.[86,87,88] This effect, simply speaking, is arising from the difference of the solvent molecule arrangement around the target materials in the ground-state and the excited state, in other words, different interaction between solvent and the dipole moment of the target. The emission energy shift is generally evaluated with a relation, $\Delta E \propto -(\alpha_e-\alpha_g)[f(\varepsilon_e)- f(n^2)]$ where α_e and α_g are the polarizability of the excited state and the ground state, respectively, and $f(x) = 2(x-1)/(2x+1)$ is the Onsager polarity function.[89] What they observed is that, as $f(\varepsilon_e)- f(n^2)$ increased the PL emission showed redshifts, which indicates the excited state was more stabilized in polar solvents. However, in the case of halogenated solvents, the PL showed blueshifts and a large enhancement in the intensity. They claimed that this was attributed to p-type doping effect from the halogen. Also reference 82 described the solvent effect from the viewpoint of the dielectric screening as shown in **Figure 15**-(c). Similarly, they investigated the excitonic PL behavior of SL-MoS_2 prepared from chemical vapor deposition against various organic solvents. To avoid the doping effects, non-ionic organic solvents such as methanol and toluene were utilized. They found that the PL showed blue shifts as a function of the dielectric constant of the solvent and that the trion/exciton intensity ratio was largely modulated. They claimed that this can be attributed to the dielectric screening of the Coulomb interactions either between electrons and holes or

among electrons. Both cases can give rise to modulation of the binding energy of excitons and trions or electronic bandgap structures. To explain this effect, they developed a scaling relationship between the extracted electronic band structure and the binding energy of exciton and trion, which showed good agreement with the idea. Interestingly, they also simulated the Coulomb potential distribution of the electron-hole pair in the dielectric/MoS_2/dielectric structure and found that the Coulomb potential distribution was strongly screened by the environmental dielectrics. This dielectric screening may make the exciton Bohr radius smaller (MoS_2 is predicted to have small Bohr radius of ~ 1nm due to the strong binding energy). Besides the bright excitonic PL, TMDs are also known to show inter-Valley (optically forbidden) dark excitons, which possibly work to reveal a finger print of adsorbed poar molecules.[90] It is worth emphasizing that, as demonstrated by many researchers, the optical properties, strong light-matter interactions of MoS_2 has a great potential to sense surface specific events and to reveal the spatial distribution of the event.

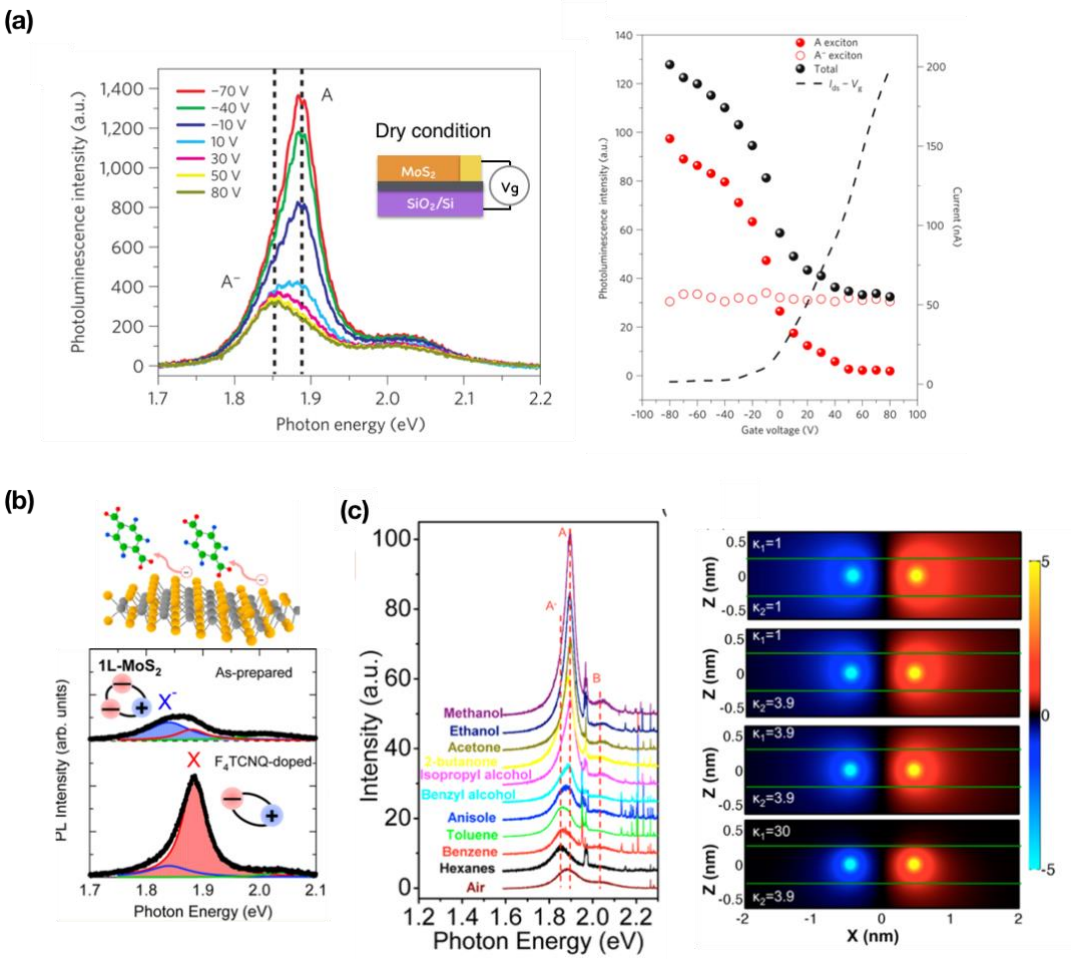

Figure 15. (a) Electrostatic modulation of the excitonic states of SL-MoS_2. Reprinted with permission from ref. 78. (b) PL modulation of SL-MoS_2 by adsorbed p-type and n-type chemical dopants. Reprinted with permission from ref. 80. Copyright 2013 American Chemical Society. (c) PL spectra of SL-MoS_2 under various organic solvents and Coulomb potential distributions of a pair of a positive charge and negative charge in the dielectric sandwiched structure. Reprinted with permission from ref. 82. Copyright 2014 American Chemical Society.

1.5 References

[1] G. Meyrink, E. Bleiler, The Golem, Dover Publications, Mineola NY 1986./ M. Shelley , Frankenstein , Oxford University Press , New York 2009 .

[2] Fromherz, P.; Offenhausser, A.; Vetter, T.; Weis, J. A Neuron-Silicon Junction: A Retzius Cell of the Leech on an Insulated-Gate Field-Effect Transistor. *Science* **1991**, *252* (5010), 1290–1293.

[3] Fromherz, P.; Stett, A. Silicon-Neuron Junction: Capacitive Stimulation of an Individual Neuron on a Silicon Chip. *Phys. Rev. Lett.* **1995**, *75* (8), 1670–1673.

[4] Cui, Y.; Wei, Q.; Park, H.; Lieber, C. M. Nanowire Nanosensors for Highly Sensitive and Selective Detection of Biological and Chemical Species. *Science* **2001**, *293* (5533), 1289–1292.

[5] Ouyang, M.; Huang, J.; Lieber, C. M. Fundamental Electronic Properties and Applications of Single-Walled Carbon Nanotubes. *Acc. Chem. Res.* **2002**, *35* (12), 1018–1025.

[6] Patolsky, F.; Timko, B. P.; Yu, G.; Fang, Y.; Greytak, A. B.; Zheng, G.; Leiber, C. M. Detection, Stimulation, and Inhibition of Neuronal Signals with High-Density Nanowire Transistor Arrays. *Science* **2006**, *313* (5790), 1100–1104.

[7] Geim, A. K. Graphene: Status and Prospects. *Science* **2009**, *324* (5934), 1530–1534.

[8] Geim, A. K.; Novoselov, K. S. The Rise of Graphene. *Nat. Mater.* **2007**, *6* (3), 183–191.

[9] Ohno, Y.; Maehashi, K.; Yamashiro, Y.; Matsumoto, K. Electrolyte-Gated Graphene Field-Effect Transistors for Detecting PH and Protein Adsorption. *Nano Lett.* **2009**, *9* (9), 3318–3322.

[10] Lu, C.-H.; Yang, H.-H.; Zhu, C.-L.; Chen, X.; Chen, G.-N. A Graphene Platform for Sensing Biomolecules. *Angew. Chemie Int. Ed.* **2009**, *48* (26), 4785–4787.

[11] Cohen-Karni, T.; Qing, Q.; Li, Q.; Fang, Y.; Lieber, C. M. Graphene and Nanowire Transistors for Cellular Interfaces and Electrical Recording. *Nano Lett.* **2010**, *10* (3), 1098–1102.

[12] Hess, L. H.; Jansen, M.; Maybeck, V.; Hauf, M. V.; Seifert, M.; Stutzmann, M.; Sharp, I. D.; Offenhäusser, A.; Garrido, J. A. Graphene Transistor Arrays for Recording Action Potentials from Electrogenic Cells. *Adv. Mater.* **2011**, *23* (43), 5045–5049.

[13] Burt, R.; Birkett, G.; Zhao, X. S. A Review of Molecular Modelling of Electric Double Layer Capacitors. *Phys. Chem. Chem. Phys.* **2014**, *16* (14), 6519–6538.

[14] Bard, A. J.; Faulkner, L. R. *ELECTROCHEMICAL METHODS: Fundamentals and Applications.*; wiley New York, 2001; Vol. 30.

[15] Wu, C. H.; Weatherup, R. S.; Salmeron, M. B. Probing Electrode/Electrolyte Interfaces in Situ by X-Ray Spectroscopies: Old Methods, New Tricks. *Phys. Chem. Chem. Phys.* **2015**, *17* (45), 30229–30239.

[16] Shen, Y. R.; Ostroverkhov, V. Sum-Frequency Vibrational Spectroscopy on Water Interfaces: Polar Orientation of Water Molecules at Interfaces. *Chem. Rev.* **2006**, *106* (4), 1140–1154.

[17] Fukuma, T.; Garcia, R. Atomic- and Molecular-Resolution Mapping of Solid–Liquid Interfaces by 3D Atomic Force Microscopy. *ACS Nano* **2018**, *12* (12), 11785–11797.

[18] Paulus, G. L. C.; Nelson, J. T.; Lee, K. Y.; Wang, Q. H.; Reuel, N. F.; Grassbaugh, B. R.; Kruss, S.; Landry, M. P.; Kang, J. W.; Vander Ende, E.; et al. A Graphene-Based Physiometer Array for the Analysis of Single Biological Cells. *Sci. Rep.* **2014**, *4*, 6865.

[19] Toma, K.; Kano, H.; Offenhäusser, A. Label-Free Measurement of Cell–Electrode Cleft Gap Distance with High Spatial Resolution Surface Plasmon Microscopy. *ACS Nano* **2014**, *8* (12), 12612–12619.

[20] Noy, A. Bionanoelectronics. *Adv. Mater.* **2011**, *23* (7), 807–820.

[21] Steinhoff, G.; Purrucker, O.; Tanaka, M.; Stutzmann, M.; Eickhoff, M. AlxGa1-XN - A New Material System for Biosensors. *Adv. Funct. Mater.* **2003**, *13* (11), 841–846.

[22] Misra, N.; Martinez, J. A.; Huang, S.-C. J.; Wang, Y.; Stroeve, P.; Grigoropoulos, C. P.; Noy, A. Bioelectronic Silicon Nanowire Devices Using Functional Membrane Proteins. *Proc. Natl. Acad. Sci.* **2009**, *106* (33), 13780–13784.

[23] Tunuguntla, R. H.; Bangar, M. A.; Kim, K.; Stroeve, P.; Grigoropoulos, C.; Ajo-Franklin, C. M.; Noy, A. Bioelectronic Light-Gated Transistors with Biologically Tunable Performance. *Adv. Mater.* **2015**, *27* (5), 831–836.

[24] Ang, P. K.; Jaiswal, M.; Haley, C.; Xuan, Y.; Wang, Y.; Sankaran, J.; Loh, K. P.; Li, A.; Lim, C. T.; Wohland, T. A Bioelectronic Platform Using a Graphene− Lipid Bilayer Interface. *ACS Nano* **2010**, *4* (12), 7387–7394.

[25] Wang, Y. Y.; Pham, T. D.; Zand, K.; Li, J.; Burke, P. J. Charging the Quantum Capacitance of Graphene with a Single Biological Ion Channel. *ACS Nano* **2014**, *8* (5), 4228–4238.

[26] Wilson, C. J.; Bommarius, A. S.; Champion, J. A.; Chernoff, Y. O.; Lynn, D. G.; Paravastu, A. K.; Liang, C.; Hsieh, M.-C.; Heemstra, J. M. Biomolecular Assemblies: Moving from Observation to Predictive Design. *Chem. Rev.* **2018**, *118* (24), 11519–11574.

[27] Mann, S. Molecular Recognition in Biomineralization. *Nature* **1988**, *332* (6160), 119–124.

[28] H. A. Lowenstam and S. Weiner, On Biomineralization (Oxford University Press, Oxford, UK, 1989).

[29] Sarikaya, M.; Tamerler, C.; Jen, A. K.-Y.; Schulten, K.; Baneyx, F. Molecular Biomimetics: Nanotechnology through Biology. *Nat. Mater.* **2003**, *2* (9), 577–585.

[30] Kowalewski, T.; Holtzman, D. M. In Situ Atomic Force Microscopy Study of Alzheimer's Beta-Amyloid Peptide on Different Substrates: New Insights into Mechanism of Beta-Sheet Formation. *Proc. Natl. Acad. Sci. U. S. A.* **1999**, *96* (7), 3688–3693.

[31] Selkoe, D. J. Alzheimer's Disease--Genotypes, Phenotype, and Treatments. *Science* **1997**, *275* (5300), 630–631.

[32] Perutz, M. Glutamine Repeats and Inherited Neurodegenerative Diseases: Molecular Aspects. *Curr. Opin. Struct. Biol.* **1996**, *6* (6), 848–858.

[33] Harper, J. D.; Wong, S. S.; Lieber, C. M.; Lansbury, P. T. An in Vitro Model for a Possible Early Event in Alzheimer's Disease. *Biochemistry* **1999**, *38* (28), 8972–8980.

[34] Brown, C. L.; Aksay, I. A.; Saville, D. A.; Hecht, M. H. Template-Directed Assembly of a de Novo Designed Protein. *J. Am. Chem. Soc.* **2002**, *124* (24), 6846–6848.

[35] Yang, G.; Woodhouse, K. A.; Yip, C. M. Substrate-Facilitated Assembly of Elastin-like Peptides: Studies by Variable-Temperature in Situ Atomic Force Microscopy. *J. Am. Chem. Soc.* **2002**, *124* (36), 10648–10649.

[36] Zhang, F.; Du, H. N.; Zhang, Z. X.; Ji, L. N.; Li, H. T.; Tang, L.; Wang, H. Bin; Fan, C. H.; Xu, H. J.; Zhang, Y.; et al. Epitaxial Growth of Peptide Nanofilaments on Inorganic Surfaces: Effects of Interfacial Hydrophobicity/Hydrophilicity. *Angew. Chem. Int. Ed.* **2006**, *45* (22), 3611–3613.

[37] Dai, B.; Kang, S. -g.; Huynh, T.; Lei, H.; Castelli, M.; Hu, J.; Zhang, Y.; Zhou, R. Salts Drive Controllable Multilayered Upright Assembly of Amyloid-like Peptides at Mica/Water Interface. *Proc. Natl. Acad. Sci.* **2013**, *110* (21), 8543–8548.

[38] So, C. R.; Hayamizu, Y.; Yazici, H.; Gresswell, C.; Khatayevich, D.; Tamerler, C.; Sarikaya, M. Controlling Self-Assembly of Engineered Peptides on Graphite by Rational Mutation. *ACS Nano* **2012**, *6* (2), 1648–1656.

[39] Cui, Y.; Kim, S. N.; Jones, S. E.; Wissler, L. L.; Naik, R. R.; McAlpine, M. C. Chemical Functionalization of Graphene Enabled by Phage Displayed Peptides. *Nano Lett.* **2010**, *10* (11), 4559–4565.

[40] Mustata, G.-M.; Kim, Y. H.; Zhang, J.; DeGrado, W. F.; Grigoryan, G.; Wanunu, M. Graphene Symmetry Amplified by Designed Peptide Self-Assembly. *Biophys. J.* **2016**, *110* (11), 2507–2516.

[41] Katoch, J.; Kim, S. N.; Kuang, Z.; Farmer, B. L.; Naik, R. R.; Tatulian, S. A.; Ishigami, M. Structure of a Peptide Adsorbed on Graphene and Graphite. *Nano Lett.* **2012**, *12* (5), 2342–2346.

[42] Kim, S. N.; Kuang, Z.; Slocik, J. M.; Jones, S. E.; Cui, Y.; Farmer, B. L.; McAlpine, M. C.; Naik, R. R. Preferential Binding of Peptides to Graphene Edges and Planes. *J. Am. Chem. Soc.* **2011**, *133* (37), 14480–14483.

[43] Akdim, B.; Pachter, R.; Kim, S. S.; Naik, R. R.; Walsh, T. R.; Trohalaki, S.; Hong, G.; Kuang, Z.; Farmer, B. L. Electronic Properties of a Graphene Device with Peptide Adsorption: Insight from Simulation. *ACS Appl. Mater. Interfaces* **2013**, *5* (15), 7470–7477.

[44] Hughes, Z. E.; Tomásio, S. M.; Walsh, T. R. Efficient Simulations of the Aqueous Bio-Interface of Graphitic Nanostructures with a Polarisable Model. *Nanoscale* **2014**, *6* (10), 5438–5448.

[45] Cohavi, O.; Corni, S.; de Rienzo, F.; di Felice, R.; Gottschalk, K. E.; Hoefling, M.; Kokh, D.; Molinari, E.; Schreiber, G.; Vaskevich, A. Protein-Surface Interactions: Challenging Experiments and Computations. *J. Mol. Recognit.* **2010**, *23* (3), 259–262.

[46] Khatayevich, D.; Page, T.; Gresswell, C.; Hayamizu, Y.; Grady, W.; Sarikaya, M. Selective Detection of Target Proteins by Peptide-Enabled Graphene Biosensor. *Small* **2014**, *10* (8), 1505–1513.

[47] Hayamizu, Y.; So, C. R.; Dag, S.; Page, T. S.; Starkebaum, D.; Sarikaya, M. Bioelectronic Interfaces by Spontaneously Organized Peptides on 2D Atomic Single Layer Materials. *Sci. Rep.* **2016**, *6* (1), 33778.

[48] Mannik, J.; Goldsmith, B. R.; Kane, A.; Collins, P. G. Chemically Induced Conductance Switching in Carbon Nanotube Circuits. *Phys. Rev. Lett.* **2006**, *97* (1), 016601.

[49] Heller, I.; Janssens, A. M.; Männik, J.; Minot, E. D.; Lemay, S. G.; Dekker, C. Identifying the Mechanism of Biosensing with Carbon Nanotube Transistors. *Nano Lett.* **2008**, *8* (2), 591–595.

[50] Sun, L.; Narimatsu, T.; Tsuchiya, S.; Tanaka, T.; Li, P.; Hayamizu, Y. Water Stability of Self-Assembled Peptide Nanostructures for Sequential Formation of Two-Dimensional Interstitial Patterns on Layered Materials. *RSC Adv.* **2016**, *6* (99), 96889–96897.

[51] Chen, J.; Zhu, E.; Liu, J.; Zhang, S.; Lin, Z.; Duan, X.; Heinz, H.; Huang, Y.; De Yoreo, J. J. Building Two-Dimensional Materials One Row at a Time: Avoiding the Nucleation Barrier. *Science* **2018**, *362* (6419), 1135–1139.

[52] Novoselov, K. S.; Mishchenko, A.; Carvalho, A.; Castro Neto, A. H. 2D Materials and van Der Waals Heterostructures. *Science* **2016**, *353* (6298), aac9439.

[53] Mak, K. F.; Shan, J. Photonics and Optoelectronics of 2D Semiconductor Transition Metal Dichalcogenides. *Nat. Photonics* **2016**, *10* (4), 216–226.

[54] Manzeli, S.; Ovchinnikov, D.; Pasquier, D.; Yazyev, O. V.; Kis, A. 2D Transition Metal Dichalcogenides. *Nat. Rev. Mater.* **2017**, *2* (8), 17033.

[55] Novoselov, K. S.; Geim, A. K.; Morozov, S. V.; Jiang, D.; Zhang, Y.; Dubonos, S. V.; Grigorieva, I. V.; Firsov, A. A. Electric Field Effect in Atomically Thin Carbon Films. *Science* **2004**, *306* (5696), 666–669.

[56] Novoselov, K. S.; Jiang, D.; Schedin, F.; Booth, T. J.; Khotkevich, V. V; Morozov, S. V; Geim, A. K. Two-Dimensional Atomic Crystals. *Proc. Natl. Acad. Sci.* **2005**, *102* (30), 10451–10453.

[57] Gmelin Handbook of Inorganic and Organometallic Chemistry (Springer-Verlag, Berlin, 1995), 8th ed., Vol. B7.

[58] Radisavljevic, B.; Radenovic, A.; Brivio, J.; Giacometti, V.; Kis, A. Single-Layer MoS_2 Transistors. *Nat. Nanotechnol.* **2011**, *6* (3), 147–150.

[59] Lauritsen, J. V.; Kibsgaard, J.; Helveg, S.; Topsøe, H.; Clausen, B. S.; Lægsgaard, E.; Besenbacher, F. Size-Dependent Structure of MoS_2 Nanocrystals. *Nat. Nanotechnol.* **2007**, *2* (1), 53–58.

[60] Splendiani, A.; Sun, L.; Zhang, Y.; Li, T.; Kim, J.; Chim, C. Y.; Galli, G.; Wang, F. Emerging Photoluminescence in Monolayer MoS_2. *Nano Lett.* **2010**, *10* (4), 1271–1275.

[61] Mak, K. F.; Lee, C.; Hone, J.; Shan, J.; Heinz, T. F. Atomically Thin MoS_2: A New Direct-Gap Semiconductor. *Phys. Rev. Lett.* **2010**, *105* (13), 136805.

[62] Jin, W.; Yeh, P.-C.; Zaki, N.; Zhang, D.; Sadowski, J. T.; Al-Mahboob, A.; van der Zande, A. M.; Chenet, D. A.; Dadap, J. I.; Herman, I. P.; et al. Direct Measurement of the Thickness-Dependent Electronic Band Structure of MoS_2 Using Angle-Resolved Photoemission Spectroscopy. *Phys. Rev. Lett.* **2013**, *111* (10), 106801.

[63] Li, T.; Galli, G. Electronic Properties of MoS_2 Nanoparticles. *J. Phys. Chem. C* **2007**, *111* (44), 16192–16196.

[64] Yin, Z.; Li, H.; Li, H.; Jiang, L.; Shi, Y.; Sun, Y.; Lu, G.; Zhang, Q.; Chen, X.; Zhang, H. Single-Layer MoS_2 Phototransistors. *ACS Nano* **2012**, *6* (1), 74–80.

[65] Lopez-Sanchez, O.; Lembke, D.; Kayci, M.; Radenovic, A.; Kis, A. Ultrasensitive Photodetectors Based on Monolayer MoS_2. *Nat. Nanotechnol.* **2013**, *8* (7), 497–501.

[66] Koppens, F. H. L.; Mueller, T.; Avouris, P.; Ferrari, A. C.; Vitiello, M. S.; Polini, M. Photodetectors Based on Graphene, Other Two-Dimensional Materials and Hybrid Systems. *Nat. Nanotechnol.* **2014**, *9* (10), 780–793.

[67] Kufer, D.; Konstantatos, G. Photo-FETs: Phototransistors Enabled by 2D and 0D Nanomaterials. *ACS Photonics* **2016**, *3* (12), 2197–2210.

[68] Sarkar, D.; Liu, W.; Xie, X.; Anselmo, A. C.; Mitragotri, S.; Banerjee, K. MoS_2 Field-Effect Transistor for Next-Generation Label-Free Biosensors. *ACS Nano* **2014**, *8* (4), 3992–4003.

[69] Lee, J.; Dak, P.; Lee, Y.; Park, H.; Choi, W.; Alam, M. a; Kim, S. Two-Dimensional Layered MoS_2 Biosensors Enable Highly Sensitive Detection of Biomolecules. *Sci. Rep.* **2014**, *4*, 7352.

[70] Wu, H.; Yang, R.; Song, B.; Han, Q.; Li, J.; Zhang, Y.; Fang, Y.; Tenne, R.; Wang, C. Biocompatible Inorganic Fullerene-Like Molybdenum Disulfide Nanoparticles Produced by Pulsed Laser Ablation in Water. *ACS Nano* **2011**, *5* (2), 1276–1281.

[71] Nair, P. R.; Alam, M. A. Screening-Limited Response of NanoBiosensors. *Nano Lett.* **2008**, *8* (5), 1281–1285.

[72] Lee, K.; Nair, P. R.; Scott, A.; Alam, M. A.; Janes, D. B. Device Considerations for Development of Conductance-Based Biosensors. *J. Appl. Phys.* **2009**, *105* (10), 102046.

[73] Cheiwchanchamnangij, T.; Lambrecht, W. R. L. Quasiparticle Band Structure Calculation of Monolayer, Bilayer, and Bulk MoS_2. *Phys. Rev. B* **2012**, *85* (20), 205302.

[74] Qiu, D. Y.; da Jornada, F. H.; Louie, S. G. Optical Spectrum of MoS_2: Many-Body Effects and Diversity of Exciton States. *Phys. Rev. Lett.* **2013**, *111* (21), 216805.

[75] Berkelbach, T. C.; Hybertsen, M. S.; Reichman, D. R. Theory of Neutral and Charged Excitons in Monolayer Transition Metal Dichalcogenides. *Phys. Rev. B - Condens. Matter Mater. Phys.* **2013**, *88* (4), 045318.

[76] Zhang, C.; Johnson, A.; Hsu, C.-L.; Li, L.-J.; Shih, C.-K. Direct Imaging of Band Profile in Single Layer MoS_2 on Graphite: Quasiparticle Energy Gap, Metallic Edge States, and Edge Band Bending. *Nano Lett.* **2014**, *14* (5), 2443–2447.

[77] Haug, H. & Koch, S. W. Quantum Theory of the Optical and Electronic Properties of Semiconductors (World Scientific, 2004). Text book

[78] Mak, K. F.; He, K.; Lee, C.; Lee, G. H.; Hone, J.; Heinz, T. F.; Shan, J. Tightly Bound Trions in Monolayer MoS_2. *Nat. Mater.* **2013**, *12* (3), 207–211.

[79] Ross, J. S.; Wu, S.; Yu, H.; Ghimire, N. J.; Jones, A. M.; Aivazian, G.; Yan, J.; Mandrus, D. G.; Xiao, D.; Yao, W.; et al. Electrical Control of Neutral and Charged Excitons in a Monolayer Semiconductor. *Nat. Commun.* **2013**, *4*, 1473–1476.

[80] Mouri, S.; Miyauchi, Y.; Matsuda, K. Tunable Photoluminescence of Monolayer MoS_2 via Chemical Doping. *Nano Lett.* **2013**, *13* (12), 5944–5948.

[81] Mao, N.; Chen, Y.; Liu, D.; Zhang, J.; Xie, L. Solvatochromic Effect on the Photoluminescence of MoS_2 Monolayers. *Small* **2013**, *9* (8), 1312–1315.

[82] Lin, Y.; Ling, X.; Yu, L.; Huang, S.; Hsu, A. L.; Lee, Y. H.; Kong, J.; Dresselhaus, M. S.; Palacios, T. Dielectric Screening of Excitons and Trions in Single-Layer MoS_2. *Nano Lett.* **2014**, *14* (10), 5569–5576.

[83] Thilagam, A. Two-Dimensional Charged-Exciton Complexes. *Phys. Rev. B* **1997**, *55* (12), 7804–7808.

[84] Coletti, C.; Riedl, C.; Lee, D. S.; Krauss, B.; Patthey, L.; von Klitzing, K.; Smet, J. H.; Starke, U. Charge Neutrality and Band-Gap Tuning of Epitaxial Graphene on SiC by Molecular Doping. *Phys. Rev. B* **2010**, *81* (23), 235401.

[85] Chen, W.; Chen, S.; Qi, D. C.; Gao, X. Y.; Wee, A. T. S. Surface Transfer P-Type Doping of Epitaxial Graphene. *J. Am. Chem. Soc.* **2007**, *129* (34), 10418–10422.

[86] Reichardt, C. Solvatochromic Dyes as Solvent Polarity Indicators. *Chem. Rev.* **1994**, *94* (8), 2319–2358.

[87] Leatherdale, C. A.; Bawendi, M. G. Observation of Solvatochromism in CdSe Colloidal Quantum Dots. *Phys. Rev. B* **2001**, *63* (16), 165315.

[88] Choi, J. H.; Strano, M. S. Solvatochromism in Single-Walled Carbon Nanotubes. *Appl. Phys. Lett.* **2007**, *90* (22), 223114.

[89] Suppan, P. Invited Review Solvatochromic Shifts: The Influence of the Medium on the Energy of Electronic States. *J. Photochem. Photobiol. A Chem.* **1990**, *50* (3), 293–330.

[90] Feierabend, M.; Berghäuser, G.; Knorr, A.; Malic, E. Proposal for Dark Exciton Based Chemical Sensors. *Nat. Commun.* **2017**, *8*, 14776.

CHAPETR 2. An Electrochemical Approach to Control the Peptide Self-Organization Behavior on a Graphite Surface

2.1 Introduction

Functionalization of solid surfaces with proteins have been widely studied aiming to develop biofuel cells,[1] biomedical devices for immunoassay,[2] drug delivery,[3] bio-sensors,[4,5,6] and protein arrays for proteomics.[7] Among possible approaches, self-organization of proteins on solid surfaces is one of promising candidates for construction of well-designed versatile interfaces with tailored structures of proteins. Many proteins have been demonstrated to form ordered structures at the nanoscale.[8]

As a substitute for using these complex proteins, peptides have recently gained much attention as convenient molecular building blocks for controlled formation of the functionalized interfaces.[9,10] Peptides selected by phage display method have been demonstrated to form self-organized structure on graphite, mica, and also gold.[11,12,13,14,15]

Among them, graphite-binding peptides (GrBPs), which were originally selected by phage display method, have been intensively utilized to understand the long-range self-organization behavior. Simple replacements of a couple of amino acids in the sequence cause major change for its binding and morphology in the peptide nanostructures, *e.g.*, a confluent film, nanowires, and nano-islands, that subsequently form on the surface.[15] By mutating the amino acid sequence, GrBPs gain the ability to form the self-organized structure on various two-dimensional nano-materials, such as graphene (semi-metal), BN (insulator), and also MoS_2 (semi-conductor).[16,17] These observations suggest that partial changes in the sequence affect the fundamental surface processes of the peptides, *i.e.*, binding, diffusion, and interactions among the peptides, leading eventually to the formation of ordered structures.

While modifications in amino acid sequence has offered fruitful information on the surface behavior of peptides as mentioned above, attempts to develop an external way to regulate the surface behavior of peptides have rarely been done. On the surface of electronic materials, an electrochemical control of the surface charge by an applied voltage appears to be a favorable way to control the behavior of the peptides. So far, many studies on protein adsorption controlled through the electrochemical approach have been done.[18,19] However, there is no experimental investigation for the electrochemical control of the long-range-ordered self-organization of proteins or peptides on atomically flat solid surfaces.

In this chapter, the correlation of peptides sequences with their organization on the solid surface in the response on the electrochemically applied surface potential has been investigated, aiming to obtain a potential design rule for peptide-functionalized interface. In particular, the net charge of peptides and the position of the charged amino acids in the sequence, either in the intermolecular interaction domain or in the surface-binding domain, were examined to obtain better understanding on the surface behavior of peptides in forming ordered or disordered structures.

As illustrated in **Figure 1**, there are two important interactions during the process of peptide self-organization on the solid surface to be considered: (1) peptide/surface interaction (Ips) for binding and diffusion (regime I) and (2) peptide/peptide interaction on the surface

(Ipp) for aggregation or ordering (regime II). The above interactions presumably contain a combination of (i) long-range interactions, *i.e.*, electrostatic forces and templating by the solid, and (ii) short-range interactions, i.e., van der Waals forces, salt bridges, and hydrogen bonding. The question here is how the surface potential affects these surface phenomena through the modulation of these interactions by mutating the peptide at specific positions in the sequence.

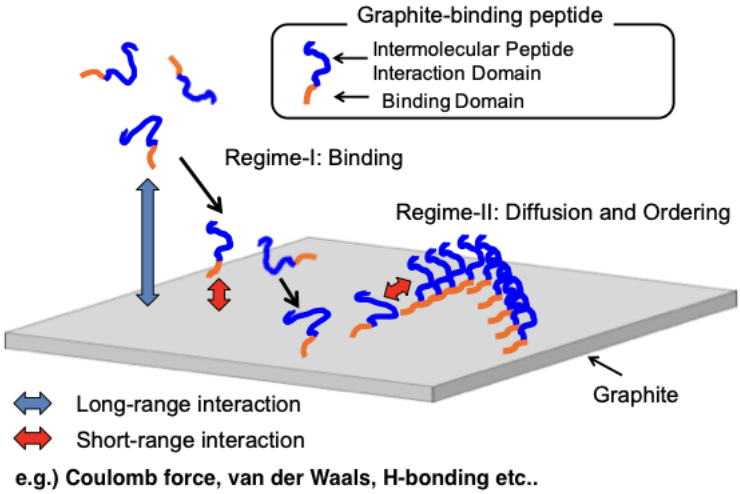

Figure 1. Schematic illustration depicting possible interactions during the peptide self-organization process on the solid surface. Regimes I and II show two main processes: (I) binding to the solid surface and (II) subsequent diffusion and ordering.

2.2 Design of amino acid sequence of self-assembled peptides

To address the question mentioned above, I synthesized several variants of GrBP5-WT as shown in **Table 1**. These peptides sequences were rationally designed as below. Both WT and M6 peptides are negatively charged in pure water (pH 7) according to expected pKa values of glutamic acid and aspartic acid. In the original sequence of WT peptide, two carboxylic acid side chains, glutamic acid, and aspartic acid are located in the middle of the peptide sequence. The domain containing carboxylic acids is expected to have dominant effects on interactions between neighboring peptides. In the sequence of M6 peptide, two acidic residues (negatively charged side chains) were moved in between the two tyrosine-aromatic residues near the C-terminus. Since these tyrosines are attributed to strong binding to graphite surface *via* π-π interaction, I envision enhanced interactions between graphite surface and the charged amino acids in between tyrosines. M8 is a positive version of M6. In the sequence of M8 peptide, the two carboxylic acids in M6 were replaced with two basic arginine residues (positively charged side chains). In the case of M9 peptide, the two acidic residues in the WT peptide were replaced with their noncharged amide equivalents (glutamic acid to glutamine, aspartic acid to asparagine). Finally, in the N-WT sequence, one acidic residue was replaced with a basic residue (glutamic acid to lysine) to be a net-neutral zwitterionic peptide at neutral pH in water.

Table 1. Amino acids sequence of self-organized peptides used in this work

Name	Amino acid (AA) sequence												MW	Net Charge
	1	2	3	4	5	6	7	8	9	10	11	12		
GrBP5(WT)	I	M	V	T	E	S	S	D	Y	S	S	Y	1381.4	-2
GrBP5(M6)	I	M	V	T	A	S	S	A	Y	D	D	Y	1335.4	-2
GrBP5(M8)	I	M	V	T	A	S	S	A	Y	R	R	Y	1417.6	+2
GrBP5(M9)	I	M	V	T	Q	S	S	N	Y	S	S	Y	1379.5	0
Neutral-WT (N-WT)	I	M	V	T	K	S	S	D	Y	S	S	Y	1380.5	0

2.3 Peptide self-assembly under electrochemical bias and evaluation method of electrochemical effects on peptide self-assembly

To investigate the electrochemical effect, a simple electrochemical cell was assembled with highly ordered pyrolytic graphite (HOPG) as the working electrode and a Pt wire as the counter electrode (**Figure 2-(a)**). The HOPG substrate (SPI-1) was purchased from the SPI supplies and cleaved before the usage to maintain a clean surface for peptide self-assembly. Peptide solution was prepared by dissolving a lyophilized peptide powder in Milli-Q water. First, a droplet of peptide solution (30 µL) was placed on the freshly cleaved HOPG substrate, and a Pt electrode was immediately inserted into the droplet. Then, a constant voltage was applied between the substrate and the Pt electrode *via* a potentiostat. The sample was incubated at room temperature for 1 hour under a humidified atmosphere to prevent the evaporation of the droplet. After incubation, the droplet was gently removed with nitrogen gas blow, and any remaining water was evaporated by continuous blowing with dry nitrogen gas for about 20 s. After the HOPG surface were dried up sufficiently, the morphological features of self-organized peptides on the surface was characterized by atomic force microscopy (AFM). An electrochemical window was also investigated with HOPG/water/Pt system. Using cyclic voltammetry method, the current between the HOPG electrode and the Pt electrode remained ±20 nA in the range of -1.0 to +0.5 V (**Figure 2-(b)**). In this range, the leak current through the solution was negligible so that this electrochemical interface possibly works as a capacitor. I used this electrochemical window to modulate the surface potential of the HOPG.

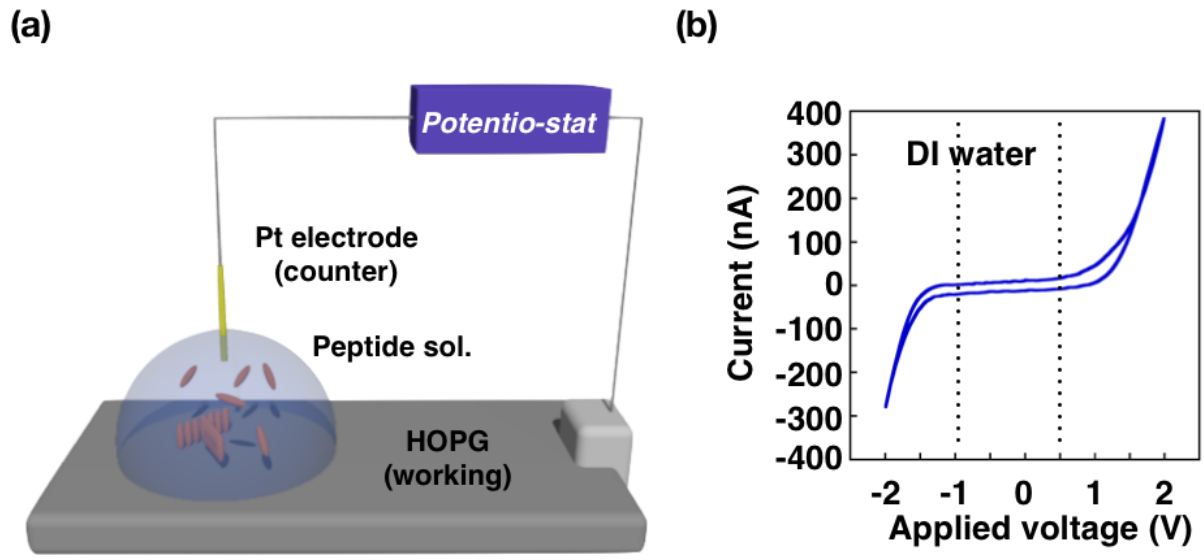

Figure 2. (a) Experimental setup for the electrochemical control of peptide self-organization on the graphite electrode surface. The setup is composed of freshly cleaved HOPG, a potentiostat, and a Pt electrode. (b) Cyclic voltammogram of the HOPG/DI water/Pt system with a voltage sweep rate of 10 mV/s.

2.4 Investigation on initial binding behavior of self-assembled peptides

Before investigating effects of an electrochemical bias to the self-assembling behavior, first the self-organization of each peptide was examined by incubating peptide solution on HOPG for 1 hour without connecting the electrode with graphite (Open circuit condition, OC). To focus on initial binding of peptides to the graphite surface, I utilized a peptide solution with a low concentration of 0.1 μM to limit probable collisions in between peptides on the surface as much as possible.

In the previous report,[21] it was found that this low concentration allows the WT peptide to form isolated islands or clusters on the surface instead of the ordered nanostructures which can be formed at higher concentrations. AFM measurements of HOPG samples incubated in 0.1 μM of WT, M6, M8, M9, and N-WT reveal surface coverages of 36, 14, 48, 23, and 17%, respectively (**Figure 3**). This indicates a significant effect of the peptide sequences on their binding affinity to the surface. Following the open circuit experiment, I performed the incubation of peptides with the Pt electrode at zero voltage (closed circuit). The surface structure of all self-organized peptides revealed similar morphological features to those obtained under OC conditions (**Figure 3**). The morphological similarities probably arise from their similar surface potentials in each case. The OC voltage of the Pt/water/HOPG system was −0.23 V, which is close to 0 V (**Figure 4**).

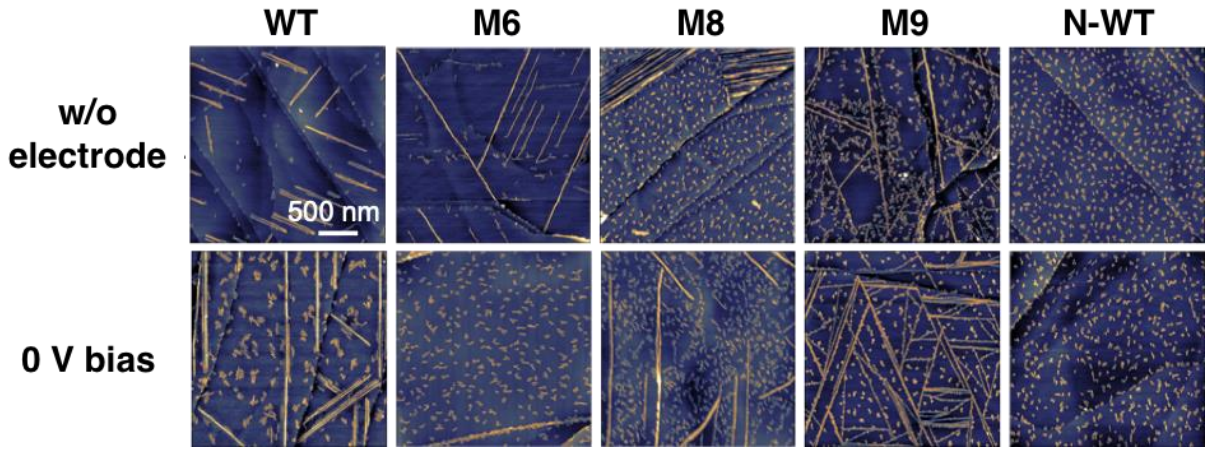

Figure 3. AFM images of the peptide organizations under open circuit (OC) and 0 V conditions with a peptide concentration of 0.1 μM in each case. AFM images were recorded under dry conditions after blowing with nitrogen.

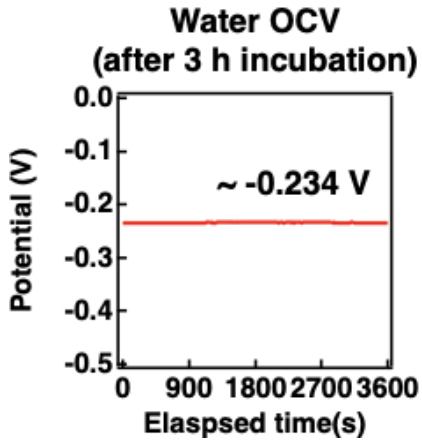

Figure 4. Time dependence of the open circuit voltage of the Pt/DI-water/HOPG system.

It was found that, depending on the net charge in each peptide sequence, the peptides showed different response to applied voltages (**Figure 5**). Based on AFM measurements carried out with a low concentration of peptides solution, *i.e.*, 0.1 μM, I derived the surface coverage of self-assembled peptides depending on the applied voltage and identified three different groups in the trend of the peptide surface coverage against the applied voltage in the range of −1.0 to 0.5 V (**Figure 6**). While negatively charged peptides, *e.g.*, WT and M6, monotonically increase their surface coverage, positively charged peptide (M8) decreases its surface coverage. The surface coverages of WT, M6, and M8 were modulated from 12, 6, and 35% to 24, 24, and 15%, respectively, with the increase in the applied voltage from −1 V to +0.5 V.

On the other hand, two neutral peptides, *e.g.*, M9 and N-WT, show almost constant coverage throughout the range of the applied voltage. These results can be simply explained

by electrostatic attractive or repulsive forces between peptides and the surface, which can be proportionally varied with the change in the surface potential. The charged peptides can be largely affected by the surface potential through the electrostatic interaction with the surface, which leaded to the variation in the flux of peptides from the bulk solution to the surface. On the contrary, the net neutral peptides were not affected by the modulation of the surface potential. Interestingly, M9 peptide containing non-charged amino acids bearing amide moiety, displays similar morphological features over the applied voltages with an almost constant coverage. Although dot like amorphous structures were observed at a voltage of more than 0 V, under 0V, M9 peptide tends to form linear nanowires. To form nanowires, *i.e.*, long-range organized structures, peptides were required to diffuse on the surface sufficiently. The observed transition in the surface behavior from nanowire-formation to dot-formation indicated that peptide binding to the surface was strongly enhanced by increasing the surface potential more than 0 V.

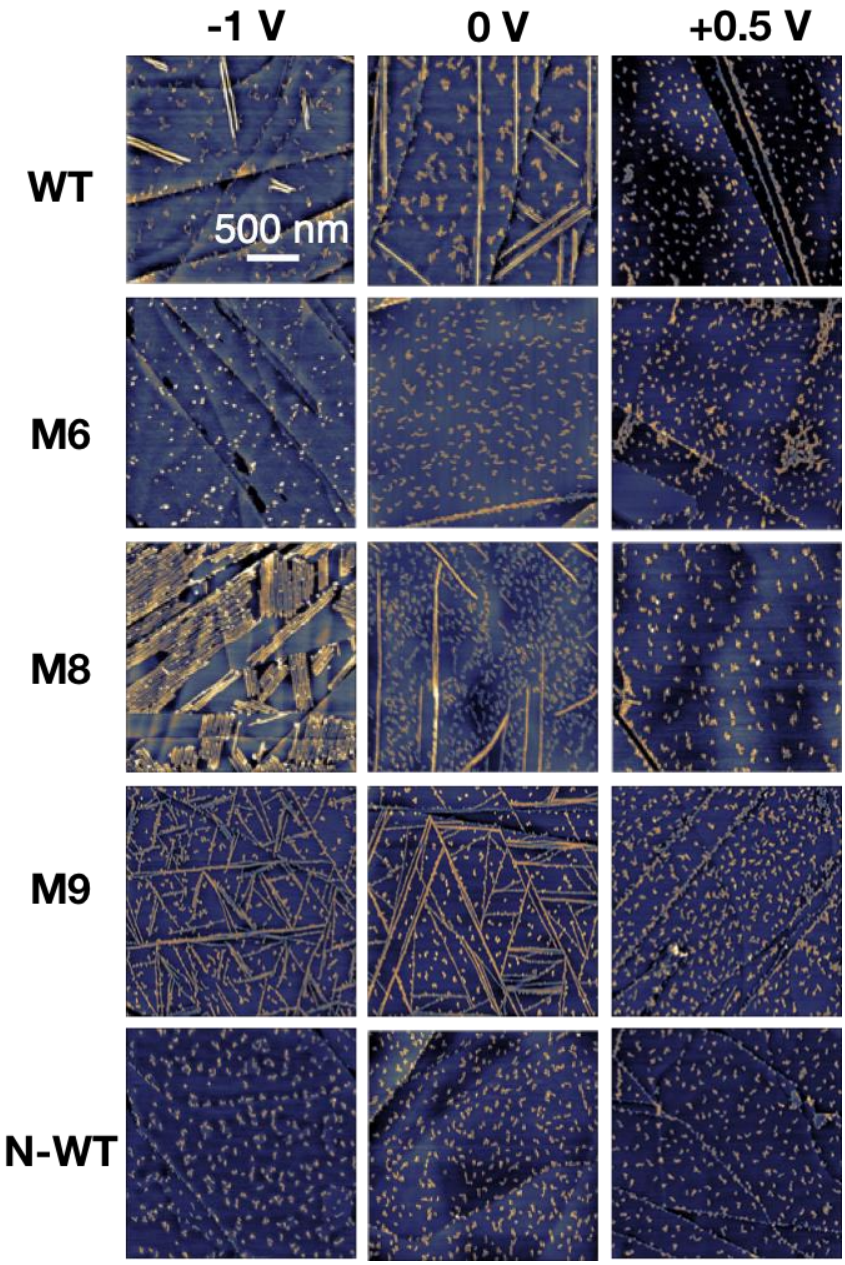

Figure 5. AFM height images of peptide organization upon applying voltage from −1.0 to +0.5 V at a low flux rate (low concentration of 0.1 μM). The color bar range of images is 3 nm. All AFM images were recorded under dry conditions.

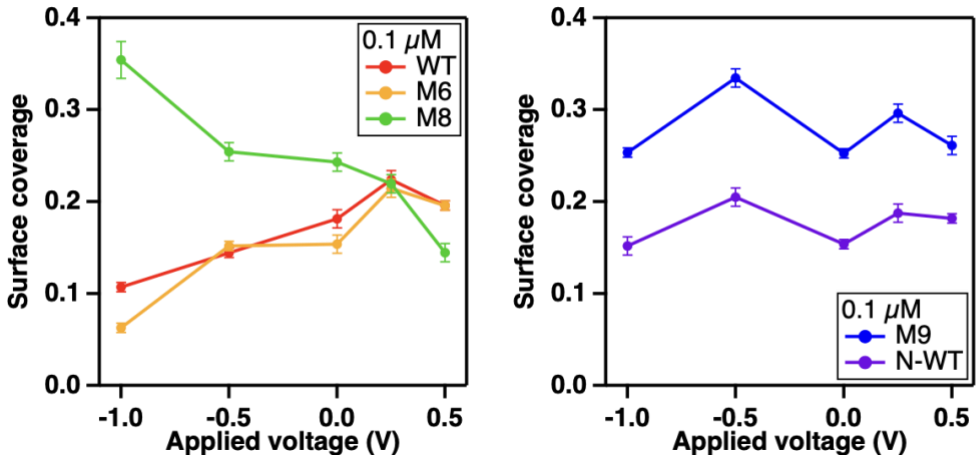

Figure 6. These plots represent the surface coverage of self-organized peptides derived from dry-condition AFM images as a function of the applied voltage.

2.5 Investigation on structural characteristics of self-organized peptides at the surface

For further investigation into the peptides' response to the applied bias in the morphological feature, a higher concentration (1.0 μM) of peptides was utilized. Focusing on the effect of charges in the sequence, negatively charged peptides (WT and M6) and positively charged peptide (M8) were studied here. In contrast to low-concentration (0.1 μM) experiments where peptide-peptide interactions *via* possible collisions among peptides were limited, I expected that intermolecular peptide-peptide interactions could have a more significant effect on the organization behavior with a higher concentration peptide solution. AFM observations, indeed, revealed more complex morphological features in response to the applied voltage than the ones with a low concentration peptide in the solution (**Figure 7**).

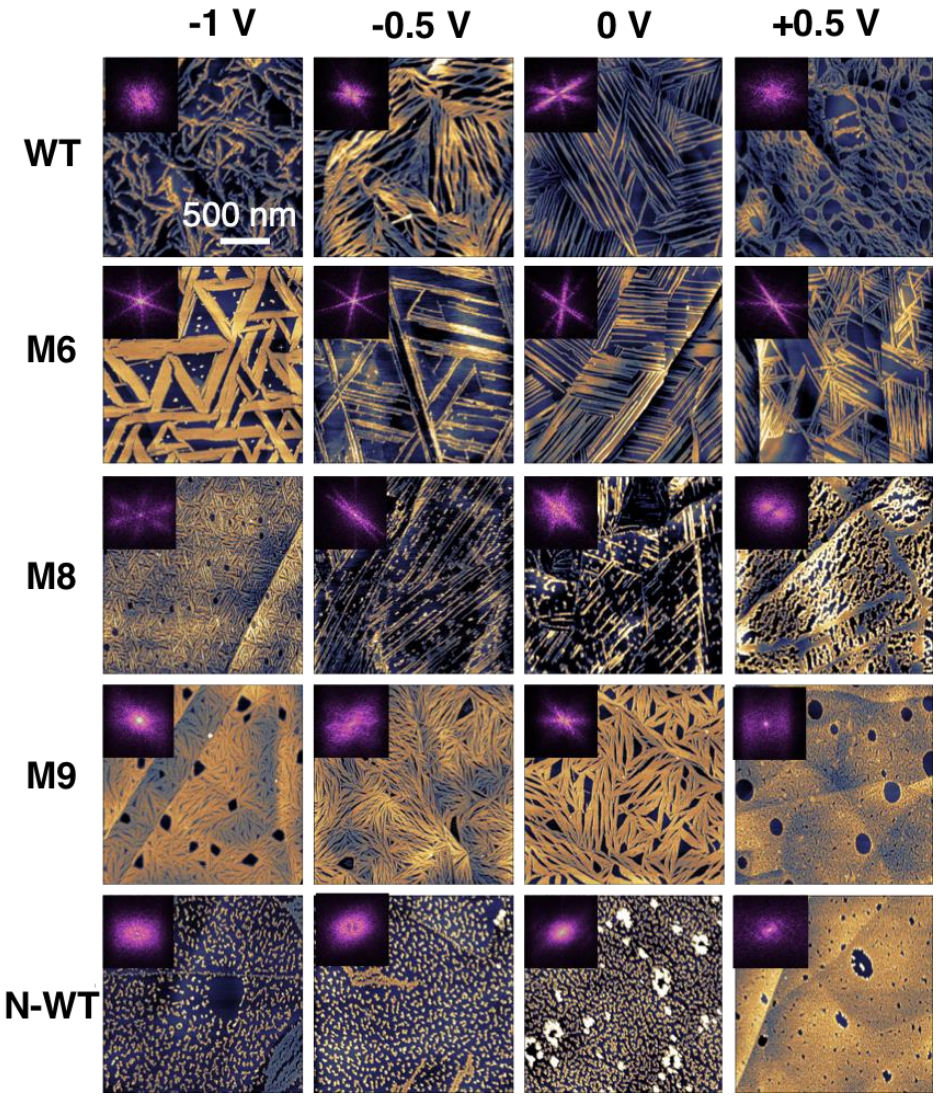

Figure 7. AFM images of self-organization behavior of the peptides at various applied voltages with a peptide concentration of 1 μM. The inset in each image is the FFT pattern corresponding to the assembly of the specific peptide under the bias shown. All AFM images were recorded under dry conditions.

First, WT and M6 showed significant morphological differences regardless of the same net charge characteristic. In the range of −1.0 to −0.5 V, WT formed a dendritic structure. Although WT and M6 created well-ordered structures in the form of more straight, robust nanowires at 0 V, WT peptide lacked linear feature in the self-organized structure and displayed wavy structure at positive bias (more than 0V) instead. The M6 peptide, however, tends to form well-ordered structures through the voltage range used.

The M8 peptide exhibited a significantly different morphological characteristics compared to those seen with the M6 peptide under these bias conditions. Although well-ordered structures were seen at large negative bias such as −1 V, this surface structure underwent significant changes at −0.5 V bias, and the nanowire structure further broke down at 0 V, long-range order disappears. The peptide formed only disordered structure at +0.5 V.

These breakdown of the long-range organized structure of peptide is associated fast Fourier transforms in the insets.

It is also interesting that the well-ordered domains have coarser feature in size, that is, the domains of M6 are wider and longer than those seen for M8 at -1V. The domain structure and the behavior of the long-range-ordered structures of M6 and M8 are understood by considering the affinity of the peptides for the surface involving electrostatic interaction, especially when the charged amino acids are in the binding domain. Because of electrostatic interactions, the increased flux of the peptides to the surface is likely to increase the nucleation density of the peptide clusters. Despite the fact that M6 and M8 have oppositely charged nature, the electrostatic force between peptides and the surface appears to be increased when an electrical bias is applied to HOPG. Furthermore, the peptide is not likely to diffuse on the surface, resulting in the formation of many domains with finer dimensions.

The behavior of M9, the neutral peptide, is quite different from that of all of the other peptides, which have positive or negative charges, in the fact that the surface coverage is highest among all and the ordered structures with relatively smaller domains survive until the bias becomes positive. Contributions of both the flux of the peptide to the surface and its subsequent diffusion of the peptides on the surface result in a large surface coverage of the organized structure. When the positive bias is applied, the surface coverage is almost complete, but without the ordered structure. This may be because the peptides have less opportunity to diffuse, refold, and interact properly with neighboring peptides to form solid-induced ordering due to too large flux of peptides immobilized on the surface.

The behavior of zwitterionic charge-neutral N-WT peptide is also characteristic. It is interesting that it never forms well-ordered structures on the surface and that the surface coverage is slightly increased over the bias range from −1 to 0 V. When the sign of bias turns to positive, the surface coverage of N-WT reaches to a comparable value to the case of M9. N-WT never shows ordered domains or linear structures but displays randomly oriented short wires and curved clusters. The formation of disordered structure by the N-WT peptides throughout the whole bias range may be attributed to the zwitterionic nature of the N-WT.

This tendency has been found in the other type of zwitterionic peptides, which is experimentally selected as a gold-binding peptide, AuBP1. This dodecapeptide has also a zwitterionic nature in the sequence and does not have the ability to form ordered structures on a graphite surface (**Figure 8**). It is assumed that zwitterionic moieties tends to form intramolecular bond, which may reduce the possibility of intermolecular interaction essential to form the organized structure.

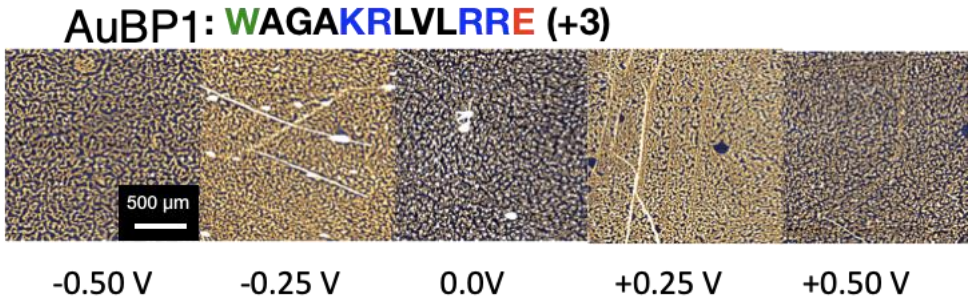

Figure 8. AFM images of self-organization behavior of the gold-binding peptides at various applied voltages with the peptide concentration of 1µM.

It is important to reemphasize that the size of the ordered domains and the nanowires shows a characteristic tendency responding to the applied voltage in all cases, in particular, in the cases of M6 and M8. According to a general concept of surface molecular assembly, the size of molecular aggregates/clusters on a surface can be inversely increased to the flux rate of the adsorbates: a lower flux rate affords a larger domain/grain size.[20] The observation for M6 and M8 exactly follows this concept, which could result from the variation in the flux rate controlled by the applied bias.

To the best of my knowledge, this is the first demonstration of controlling peptide self-organization into long-range-ordered structures in an electrochemical manner. The electrochemical control of the flux rate can be useful in the formation of nanostructures by self-assembled peptides, especially in forming long and thin well-ordered nanostructures on the electronic materials.

2.6 Investigation on surface coverage of self-organized peptides

Next, I obtained the surface coverage of peptide nano-structures from AFM observation to evaluate the correlation of coverage *vs* applied voltage from the AFM observations. Obviously, the result with the high concentration did not show a monotonic modulation of coverage by the voltage in all cases (**Figure 9**).

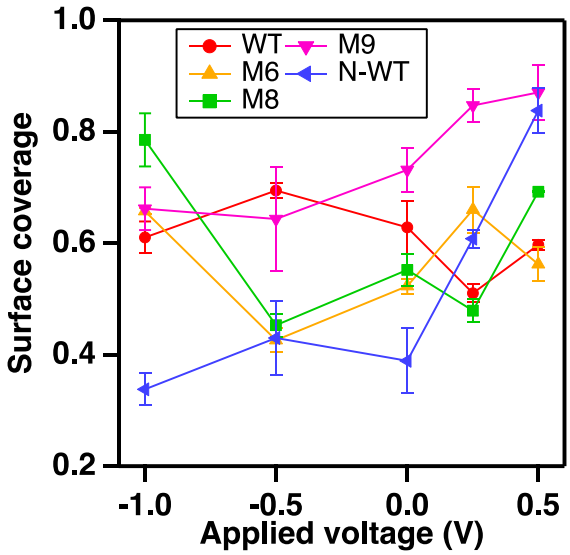

Figure 9. Plot of the surface coverage of each peptide *vs* the applied voltage at high concentration (1μM).

Here, interestingly, according to the behavior of surface coverage in response to applied bias, these five peptides can be identified into three groups: (group i) WT, (group ii) M6 and M8, and (group iii) M9 and N-WT.

The group (i) shows small variations in the coverage over the range of applied voltage. This is likely due to the reasons that the binding strengths and surface diffusion rates of the peptides do not change but the molecular interactions do change, leading to the differences only in their ordering behavior on the surface. While the group (ii) shows high coverage at large voltages (−1 and 0.5 V) but low coverage at small voltages (−0.5 and 0 V), the group (iii) shows an increase in coverage in the range of positive applied voltages. These tendencies can be closely correlated to the net charge of each peptide depending on their local pH in the vicinity of the graphite surface.

Figure 10 shows a plot of the net charge of each peptide at different pH on the basis of the pKa value of each amino acid in the peptide sequence.[18] The charge of the peptides with solution pH clearly shows that there are three types of behavior corresponding to the groups discussed above: negative, positive, and neutral peptides in the range of pH from 5 to 9. In our experiment, the peptide aqueous solution is under an equilibrium condition in air. Thus, the pH value of the bulk solution was most likely estimated to be 5.7 due to spontaneous absorption of CO_2 into the aqueous solution. Because of the protonation or deprotonation of side chains

and termini, all of the peptides can change their net charges in response to the solution pH. The local pH on the graphite surface can be varied with the applied voltage through accumulation of charged ionic species to the surface. A previous work reported the local pH of water in the vicinity of a metal surface and proposed an equation, pH = 7 ± 7.83 V, where V is the voltage applied to the metal surface.[21] On the basis of this, the local pH controlled in this work is roughly estimated to be from −1.73 to 11.4, which covers most of the range in **Figure 10**. The net charge probably affects both the intermolecular interaction among the peptides (Ipp) and the interactions between peptide and solid surface (Isp).

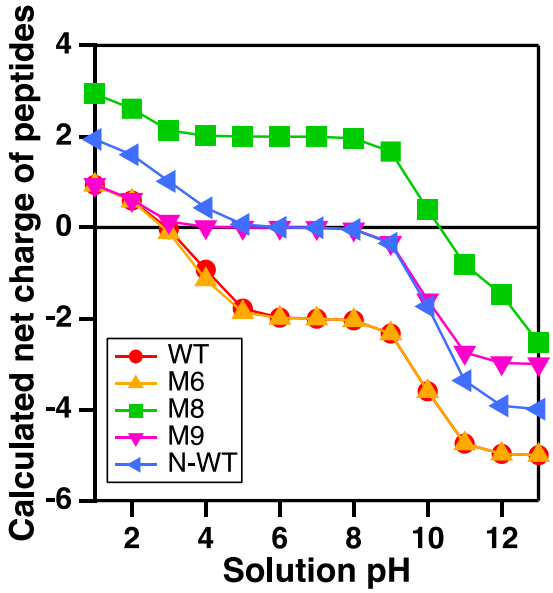

Figure 10. Calculated net charge of peptides at various pH values on the basis of pKa value of each amino acid.

Finally, to explain the morphological feature of the peptide organization and the coverage observed for each of the peptides over the range of applied voltages, **Figure 11** is provided. The schematics shows my hypothesis on the interactions of the three categories of the peptides at various surface potentials.

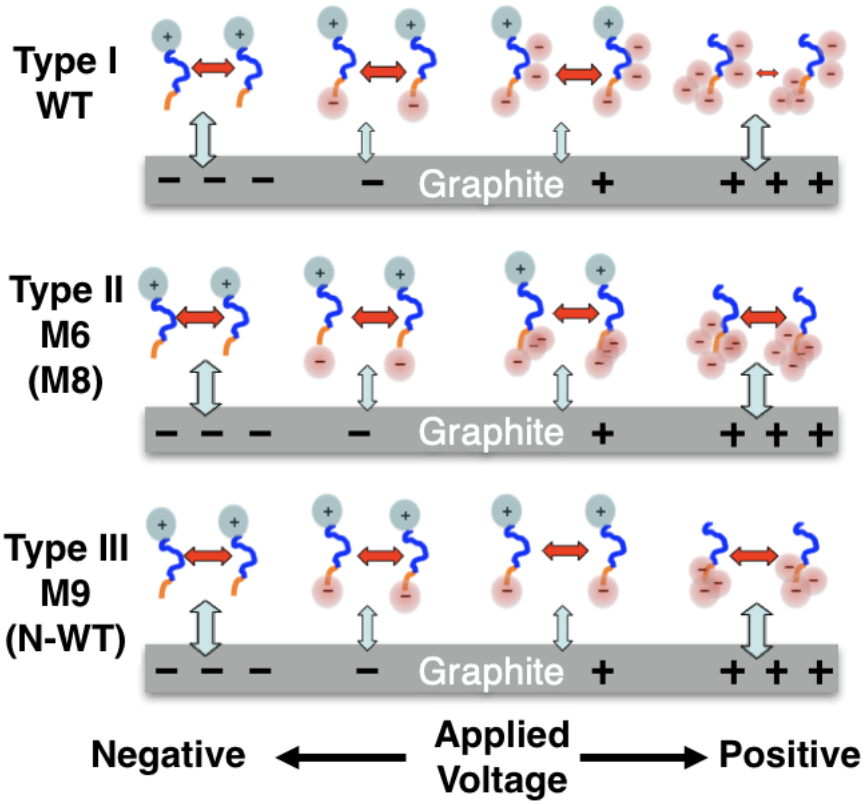

Figure 11. Schematic illustration showing charge-states of peptides at various applied voltages. Red and blue arrows indicate intermolecular interactions between the peptides (Ipp) and the peptide/surface (Ips) interactions, respectively.

Here, I focus on the kinetics of peptide self-organization on the HOPG surface. The coverage of peptides or the growth rate of the peptide nanostructures can be related to the relative values of Ipp and Isp, where, generally speaking, larger Ipp and Isp contribute to a higher coverage. The difference between groups (i) and (ii) can be explained by the position of charged amino acids. For the original WT, the first eight amino acids have an amphiphilic nature, and they have been considered to play an important role in the intermolecular interactions between peptides (Ipp), which leads to the long-range ordered structure of the peptides. On the basis of this concept, it is reasonable to assume that Ipp may be suppressed for the WT-peptides at high voltages as a result of a repulsive Coulombic force due to high net charges in peptide sequence induced by local pH modulation. Interestingly, WT is the only peptide that does not show a clear increase in coverage at high voltage.

On the other hand, M6 and M8 peptides have charged amino acids in the binding domain. Thus, these peptides are likely influenced in the Isp term, which is highly related to the final coverage, where the net charge varying with the local pH has repulsive or attractive force, respectively, on the graphite surface depending on the surface charge. At 0.5 V, the pH may reach the point where both tyrosines and the N-terminus can be deprotonated to induce negative charges. This charge regulation process probably causes too strong binding to the surface, resulting in a high coverage without linear well-ordered nanostructures.

Although peptides in group iii do not have a net positive or negative charge at pH7, the coverage increases at 0.5 V as well. It is worth mentioning that all of the peptides start losing their ability to form well-ordered structures at 1.0 V (**Figure 12**), although some (M8, M9, and N-WT) reach this at 0.5 V. This disorganization behavior may be caused by the hydrolysis of peptides under such a strong alkaline condition. In the discussion above, we considered the kinetics of the system without taking into accounts the possible variations of the local pH due to the existence of charged peptides on the surface. The local pH can vary self-consistently by the presence of the bound peptide nanostructures on the surface with a high coverage density. For further understanding, it will be necessary to establish a self-consistent computational approach in the future.

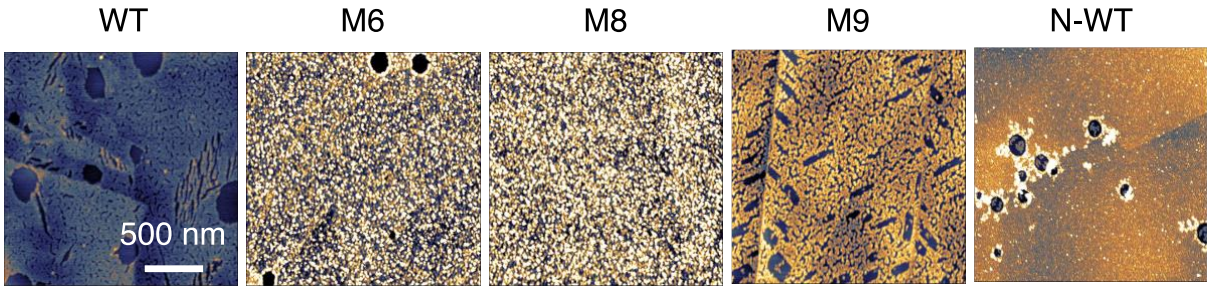

Figure 12. AFM images of self-organization behavior of the peptides at the applied voltages of 1 V with the peptide concentration of 1 µM.

2.7 Conclusion

In conclusion, the tuning of the morphological features of peptide self-organization on a graphite substrate has been successfully demonstrated by adjusting the electrochemically applied bias. At a low concentration of peptides in a solution (0.1 μM), the surface coverage of charged peptides (WT, M6, and M8) was monotonically modulated by the applied bias. On the other hand, Charge-neutral peptides (M9 and N-WT) were mostly unaffected to the applied voltage in the surface coverage. At a high concentration (1.0 μM), self-organized peptides formed well-ordered structures. The size of the peptide nanostructures has been controlled by the applied bias, probably resulting from the modulation of the flux rate of peptides by the surface potential of graphite, which has significant effects on both the surface nucleation rate and the growth rate. However, N-WT peptides with a zwitterionic nature exhibited only shorter featureless linear aggregates without the ability to form long-range ordered structures. To gain a deep insight into the surface process of peptides, further experimental and computational modeling studies at the molecular level will be required. The molecular conformation can be tightly correlated to the surface potential, which likely induces large changes in surface phenomena including the binding, diffusion, and self-organization of peptides into various nanostructures and their morphological feature. The electrochemical control presented here could allow one to design and construct peptide-based nanoscale biomolecular scaffolds on the graphite surface for future biosensing and bioelectronics applications.

In this chapter, the effect of surface potential on the organization behavior was mainly discussed to gain the insight on how the electronic states of the substrate affects the bio-molecular organization in an aqueous solution. In the following chapters, opto-electronic properties of MoS_2 as a potential substrate of bio-sensing device will be discussed.

2.8 References

[1] Halámková, L.; Halámek, J.; Bocharova, V.; Szczupak, A.; Alfonta, L.; Katz, E. Implanted biofuel cell operating in a living snail. *J. Am. Chem. Soc.* **2012**, 134 (11), 5040−5043.

[2] Seidel, M.; Niessner, R. Automated analytical microarrays: a critical review. *Anal. Bioanal. Chem.* **2008**, 391 (5), 1521−1544.

[3] Monopoli, M. P.; Walczyk, D.; Campbell, A.; Elia, G.; Lynch, I.; Baldelli Bombelli, F.; Dawson, K. A. Physical-chemical aspects of protein corona: relevance to in vitro and in vivo biological impacts of nanoparticles. *J. Am. Chem. Soc.* **2011**, 133 (8), 2525−2534.

[4] Khatayevich, D.; Page, T.; Gresswell, C.; Hayamizu, Y.; Grady, W.; Sarikaya, M. Selective Detection of Target Proteins by Peptide- Enabled Graphene Biosensor. *Small* **2014**, 10 (8), 1505−1513.

[5] Page, T. R.; Hayamizu, Y.; So, C. R.; Sarikaya, M. Electrical detection of biomolecular adsorption on sprayed graphene sheets. *Biosens. Bioelectron*. **2012**, 33 (1), 304−308.

[6] Ohno, Y.; Maehashi, K.; Matsumoto, K. Label-free biosensors based on aptamer-modified graphene field-effect transistors. *J. Am. Chem. Soc*. **2010**, 132 (51), 18012−18013.

[7] Colwill, K.; Gräslund, S.; Group, R. P. B. W. A roadmap to generate renewable protein binders to the human proteome. *Nat. Methods* **2011**, 8 (7), 551−558.

[8] De Yoreo, J. J.; Chung, S.; Friddle, R. W. In Situ atomic force microscopy as a tool for investigating interactions and assembly dynamics in biomolecular and biomineral systems. *Adv. Funct. Mater*. **2013**, 23 (20), 2525−2538.

[9] Whaley, S. R.; English, D.; Hu, E. L.; Barbara, P. F.; Belcher, A. M. Selection of peptides with semiconductor binding specificity for directed nanocrystal assembly. *Nature* **2000**, 405 (6787), 665−668.

[10] Sarikaya, M.; Tamerler, C.; Jen, A. K.-Y.; Schulten, K.; Baneyx, F. Molecular biomimetics: nanotechnology through biology. *Nat. Mater*. **2003**, 2 (9), 577−585.

[11] Kowalewski, T.; Holtzman, D. M. In situ atomic force microscopy study of Alzheimer's β-amyloid peptide on different substrates: New insights into mechanism of β-sheet formation. *Proc. Natl. Acad. Sci. U. S. A.* **1999**, 96 (7), 3688−3693.

[12] Zhang, F.; Du, H. N.; Zhang, Z. X.; Ji, L. N.; Li, H. T.; Tang, L.; Wang, H. B.; Fan, C. H.; Xu, H. J.; Zhang, Y. Epitaxial growth of peptide nanofilaments on inorganic surfaces: Effects of interfacial hydrophobicity/hydrophilicity. *Angew. Chem., Int. Ed*. **2006**, 45 (22), 3611−3613.

[13] Mustata, G.-M.; Kim, Y. H.; Zhang, J.; DeGrado, W. F.; Grigoryan, G.; Wanunu, M. Graphene symmetry amplified by designed peptide self-assembly. *Biophys. J.* **2016**, 110 (11), 2507− 2516.

[14] So, C. R.; Kulp, J. L., III; Oren, E. E.; Zareie, H.; Tamerler, C.; Evans, J. S.; Sarikaya, M. Molecular recognition and supramolecular self-assembly of a genetically engineered gold binding peptide on Au {111}. *ACS Nano* **2009**, 3 (6), 1525−1531.

[15] So, C. R.; Hayamizu, Y.; Yazici, H.; Gresswell, C.; Khatayevich, D.; Tamerler, C.; Sarikaya, M. Controlling self-assembly of engineered peptides on graphite by rational mutation. *ACS Nano* **2012**, 6 (2), 1648−1656.

[16] Kim, S. N.; Kuang, Z.; Slocik, J. M.; Jones, S. E.; Cui, Y.; Farmer, B. L.; McAlpine, M. C.; Naik, R. R. Preferential binding of peptides to graphene edges and planes. *J. Am. Chem. Soc.* **2011**, 133 (37), 14480− 14483.

[17] Hayamizu, Y.; So, C. R.; Dag, S.; Page, T. S.; Starkebaum, D.; Sarikaya, M. Bioelectronic interfaces by spontaneously organized peptides on 2D atomic single layer materials. *Sci. Rep.* **2016**, 6, 33778.

[18] Hartvig, R. A.; van de Weert, M.; Østergaard, J.; Jorgensen, L.; Jensen, H. Protein adsorption at charged surfaces: the role of electrostatic interactions and interfacial charge regulation. *Langmuir* **2011**, 27 (6), 2634−2643.

[19] Kubiak-Ossowska, K.; Mulheran, P. A. Mechanism of hen egg white lysozyme adsorption on a charged solid surface. *Langmuir* **2010**, 26 (20), 15954−15965.

[20] Barth, J. V.; Costantini, G.; Kern, K. Engineering atomic and molecular nanostructures at surfaces. *Nature* **2005**, 437 (7059), 671− 679.

[21] Morrow, R.; McKenzie, D. The time-dependent development of electric double-layers in pure water at metal electrodes: the effect of an applied voltage on the local pH. *Proc. R. Soc. London, Ser. A* **2012**, 468, 18−34. 1826

CHAPETR 3. Photoluminescence of MoS_2 modified by pH and Ions in Aqueous Solutions for Potential Biological Sensing

This chapter is not open because this chapter includes unpublished data.

CHAPETR 4. Anomalously Slow Optical Response of MoS_2 to Various Electrolyte Solutions at the Bioelectronic Interfaces Revealed by Electrochemical Pulse Modulation of Photoluminescence

This chapter is not open because this chapter includes unpublished data.

CHAPETR 5. Summary and Outlook

In the present thesis, to understand the interaction between biomolecules and quasi-particles, e.g., electron, hole, and electron-hole pair, which can be seen in optoelectronic materials under aqueous conditions, surface characteristics and optoelectronic properties of a system composed of self-organized peptides and two-dimensional layered materials has been investigated.

In chapter 2, the modulation of peptide-self-assembling behavior on a graphitic surface has been demonstrated by applying electrochemical biases. The self-assembling behavior involves binding to a surface, diffusion, and organization processes on the surface. To investigate the electrochemical effects on the initial binding behavior of peptides, peptide self-assembly was carried out using a low concentration peptide aqueous solution under various electrochemical biases. AFM measurement of the graphite surface revealed that, under these conditions, the surface coverage of charged peptides (WT, M6, and M8) was monotonically modulated along with the applied voltage. On the other hand, non-charged (net neutral) peptides (M9 and N-WT) were mostly insensitive to the electrochemical biases in terms of the surface coverage. To gain further insights on the organization behavior, self-organized structures grown with a high concentration peptide solution were investigated. The size and morphological features of peptide nanostructures were controlled by the design of amino acid sequence and the applied electrochemical bias, which was probably arising from the modulation of the peptide flux from bulk solution to the surface. The flux modulation by the electrochemical bias should have significances on both the nucleation and the growth of the nanostructures. The electrochemical control demonstrated here could allow one to design and construct peptide-based nanoscale biomolecular scaffolds on the graphite surface for future biosensing and bioelectronics applications.

The chapter 3 is not open because this chapter includes unpublished

The chapter 4 is not open because this chapter includes unpublished

Investigation on the bioelectronic interfaces consisting of the self-organized peptides and 2D nano-materials from the point of view of peptides and electronic materials suggests the existence of unique surface phenomena involved with the complex interplay among water, ions and, biomolecules. These surface phenomena will play prominent roles in the rational construction of the functional surfaces and the understanding of that will pave the way for the development of new kind of optoelectronic devices.